Tutor/s

Dra. Amparo Caubet Marin
Departament de Química Inorgànica i Orgànica, Secció de Química Inorgànica

Grau de Química

Treball Final de Grau

Synthesis and characterization of 4'-substituted-2,2':6',2"-terpyridine ruthenium (II) complexes.

Síntesis i caracterització de complexes de ruteni (II) amb lligands de 4'-substituida-2,2':6',2"-terpiridina.

Antoni Vanrell Sabater

June 2022

Universitat de Barcelona

B:KC Barcelona Knowledge Campus
Campus d'Excel·lència Internacional

Hi ha una força motriu més poderosa que el vapor, l'electricitat i l'energia atòmica: la voluntat.

Albert Einstein

Voldria donar les gràcies a la Dra. Amparo Caubet Marin, pel temps que ha dedicat al projecte, pels ànims que m'ha donat quan les coses no sortien bé, per tot el que m'ha ajudat a aprendre i sobretot pels bons moments que hem compartit.

Als companys de laboratori, per tota la ajuda que m'han proporcionat, sobretot a la Srta. Piedad Herrera. Al Dr. Manuel Martínez López per tot el material que ens ha deixat .

Als companys, professors i amics de la UIB i de la UB, per totes les hores que hem passat junts, per tot el que he après al seu costat. Especialment donar les gràcies a la millor companya de laboratori que podria haver tengut, Srta. Andrea Están García.

Don les gràcies sobre tot a la meva família i amics, perquè sense el seu suport i ànims no hauria arribat on soc ara.

REPORT

IDENTIFICATION AND REFLECTION ON THE SUSTAINABLE DEVELOPMENT GOALS (ODS)

Over the centuries, hundreds of diseases have put people's health at risk. In recent centuries, major pandemics such as the plague, influenza and the coronavirus have been devastating, killing large parts of the population. In recent decades, cancer has been one of the most commonly diagnosed diseases worldwide, with more than 9 million deaths in 2019.

This project is investigating new compounds based on ruthenium complexes to treat cancer more effectively and with less risk to the patient. The photosensitizing properties of these have been tested. The project can be included in goal 3, health, of the goals of the UN's 2030 agenda.

The project has obtained positive results in the use of the synthesized complexes as DNA destroyers. The complexes have shown good interaction with DNA in non-irradiated samples. The photosensitizing properties of these complexes when irradiated with light have given good results, with 100% DNA excision in most of the complexes.

Research could continue with biological tests, treating cells with the complexes, to see what the results are when they are irradiated and when they are not. It could go on to clinical trials, and if successful, could lead to a new drug to treat cancer.

CONTENTS

1. SUMMARY

Derivate terpyridine ligands have been synthesized, following the combination of two reactions: the Michael addition and the Kröhnke condensation, giving rise to 4'-(4-bromophenyl)-2,2':6',2"-terpyridine (**3a**) and 4'-(4-aniline)-2,2':6',2"-terpyridine (**3b**). The reaction of 4'-chloro-2,2':6',2"-terpyridine or **3a** with naphthalen-2-ylmethanol produces 4'-(naphthalen-2-ylmethoxy)-2,2':6',2"-terpyridine (**3c**) or 4'-(4-(naphthalen-2-ylmethoxy)phenyl)-2,2':6',2"-terpyridine (**3d**), respectively. These ligands react with $RuCl_3 \cdot 3H_2O$ to give ruthenium (III) complexes: $[Ru(Brtrp)Cl_3]$ (**4a**), $[Ru(Anitrp)Cl_3]$ (**4b**), $[Ru(Ntrp)Cl_3]$ (**4c**) and $[Ru(BrNtrp)Cl_3]$(**4d**). Their reduction and the substitution of the two chloride for bidentate *N,N* ligands, such as 2,2'-bipyridine, 1,10-phenanthroline or 2,2'-dipyridylamine allows to obtain [Ru(Brtrp)(bipy)Cl]Cl (**5a**), [Ru(Brtrp)(phen)Cl]Cl (**5a'**), [Ru(Brtrp)(dpa)Cl]Cl (**5a"**), and [Ru(Ntrp)(bipy)Cl]Cl (**5c**). In order to try to modify their photochemical properties, the complexes $[Ru(Brtrp)(N,N)(py)](PF_6)_2$, where *N, N* = bipy (**6a**), phen (**6a'**), dpa (**6a"**) have been obtained from (**5a-a"**) by substitution of the chlorine atom coordinated to the ruthenium for a pyridine group. Also the complexes with two terpyridine ligands $[Ru(Brtrp)_2](PF_6)_2$ (**7a**) and $[Ru(Brtrp)(Ntrp)](PF_6)_2$ (**7b**) were synthesized.

The ligands and the ruthenium (II) complexes have been characterized by infrared spectroscopy (IR), mass spectrometry, and when it has been possible, by mono- and bidimensional NMR spectroscopies. Furthermore, the determination of the absorbance of the synthesized compounds by UV-vis and their fluorescence by emission and excitation spectra were carried out.

Finally, the interaction of some of the complexes with DNA has been studied by UV-Vis and electrophoresis. The results obtained from these techniques indicate that the synthesized complexes have a covalent and/or intercalation interaction with DNA and for complexes **5a** and **7a** a moderately strong intrinsic binding constant.

Keywords: Ruthenium complexes, 4'-substitute-2,2':6',2"- terpyridine, antitumoral metal-based drugs, photodynamic therapy, photosensitizer.

2. RESUM

Lligands, derivats de la terpiridina, han estat sintetitzats a partir de la combinació de les reaccions de addició de Michael i la condensació de Kröhnke, donant lloc al 4'-(4-bromofenil)-2,2':6',2"-terpiridina (**3a**) i 4'-(4-anilina)-2,2':6'2"-terpiridina (**3b**),.La reacció del lligand la 4'-cloro-2,2':6',2"-terpiridina o el (**3a**) amb naftalen-2-ilmeatnol ha produït el 4'- (naftalen-2-ilmetoxi)-2,2':6',2"-terpiridina (**3c**) i 4'-(4-(naftalen-2-ilmetoxi) fenil)-2,2':6',2"-terpiridina (**3d**), respectivament. Aquests lligands s'han fet reaccionar amb $RuCl_3 \cdot 3H_2O$, obtenint complexes de ruteni (lll), [Ru(Brtrp)Cl_3] (**4a**), [Ru(Anitrp)Cl_3] (**4b**), [Ru(Ntrp)Cl_3] (**4c**) and [Ru(BrNtrp)Cl_3](**4d**). La seva reducció i la substitució de dos clorurs per lligands N,N-bidentats, com ara 2,2'-bipiridina, 1,10-fenantrolina i 2,2'-dipiridilamina; ham permès obtenir [Ru(Brtrp)(bipy)Cl]Cl (**5a**), [Ru(Brtrp)(phen)Cl]Cl (**5a'**), [Ru(Brtrp)(dpa)Cl]Cl (**5a"**), [Ru(Anitrp)(bipy)Cl]Cl (**5b**), [Ru(Anitrp)(phen)Cl]Cl (**5b'**) and [Ru(Ntrp)(bipy)Cl]Cl (**5c**). Per tal de modificar les seves propietats fotoquímiques, s'han obtingut els complexes [Ru(Brtpy)(*N,N*)(py)]$(PF_6)_2$, on *N,N*= bipy (**6a**), phen (**6a'**) i dpa (**6a''**), mitjançant la substitució del àtom de clor coordinat per una piridina. També es van sintetitzar els complexes de ruteni (ll) amb dues terpiridines, [Ru(Brtrp)$_2$]$(PF_6)_2$ (**7a**) i [Ru(Brtrp)(Ntrp)]$(PF_6)_2$ (**7b**).

Els lligands i els complexes s'han caracteritzat per espectroscòpia infraroja (IR) i espectrometria de masses, i quan ha estat possible per NMR mono- i bidimensional. A més a més, es va dur a terme la determinació de l'absorbància i la fluorescència dels complexes sintetitzats per mitja d'espectres UV-Vis i espectres d'emissió i excitació.

Finalment, s'ha estudiat la interacció d'alguns dels complexos amb l'ADN mitjançant espectres UV-Vis i electroforesi. Els resultats obtinguts de les dues tècniques indiquen que els complexes sintetitzats tenen una interacció covalent o d'intercalació amb l'ADN. A més a més per els complexes **5a** i **7a** s'ha obtingut una constant d'enllaç intrínseca mitjanament forta.

Paraules clau: Complexos de ruteni, 4'-substitut-2,2':6',2"-terpiridina, fàrmacs antitumorals a base de metalls, teràpia fotodinàmica, fotosensibilitzant.

3. INTRODUCTION

Cancer has emerged over the last decades as one of the deadliest diseases in the world. Despite enormous research efforts over the last decades, this disease has caused more than 19.2 million new cases and 9.9 million new deaths worldwide only in the year 2020 [1]. Traditional treatment modalities involve a combination of techniques such as chemotherapy, radiotherapy, immunotherapy, or surgery. Chemotherapy with cytotoxic anticancer agents remains the mainstay of therapy targeted at specific cellular mechanisms in disease [2]. Increasingly it is being used earlier on in a patient's treatment as an adjunct to either surgery or radiotherapy.

Cis-diamminedichloridoplatinum(II), cisplatin (Figure 1), is one of the most used drugs in cancer chemotherapy. It was prepared for the first time in 1845 by Michele Peyrone [3], while working with Magnus salt, a greenish platinum-based complex. It was not until many years later, in 1965, that its antitumor activity was discovered by chance by Barnett Rosenberg, who observed the ability of cisplatin to inhibit cell division in the E. Coli bacterium. Thus, at the end of 1978, the complex was approved by the US Food and Drug Administration as an antitumor agent and used as a drug under the name Platinol [4]. Unfortunately, cisplatin has some harmful side effects, such as nephrotoxicity (kidney damage), neurotoxicity, the appearance of resistance and low solubility in the aqueous medium, which limit its use [5],[6]. This fact has stimulated research towards the design and synthesis of new platinum compounds. Three other structurally related platinum drugs (carboplatin, nedaplatin, and oxaliplatin, Figure 1) have also entered widespread clinical use [7] but no dramatic benefits have been described for these drugs over cisplatin. Anyway, the efficacy and importance of the platinum compounds are emphasized by the fact that there is hardly any

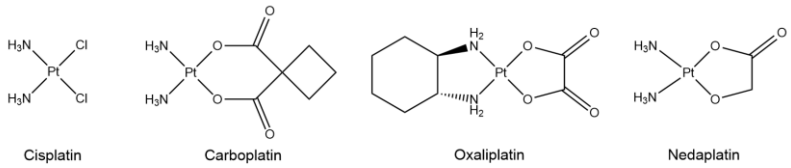

Figure 1: Structure of Cisplatin and analogues.

clinical regimen of combination chemotherapy today that does not contain cisplatin or another platinum drug [8].

Other metal complexes containing ions such as zinc (II), copper (II), gold (I), ruthenium (II) and (III) and silver (I) among others, have been also investigated and their bioactivity and antitumor capacity have been evaluated [7][8][9]. Ruthenium complexes are promising candidates that show acceptable biological properties for chemotherapy such as: (i) they are active against some cisplatin-resistant cell lines. (ii) they have low side effects due to their higher selectivity for cancer cells compared with normal cells. (iii) The higher selectivity of these compounds for their targets may be linked to selective uptake by the tumor compared with healthy tissue (iv) the ability to mimic iron in binding to some biological molecules [10].

There are currently some ruthenium (III) and ruthenium (II) compounds in various stages of clinical trials. Ruthenium therapeutic imidazolium *trans*-[tetrachlorido(DMSO)(imidazole)ruthenate(III)] (NAMI-A) (Figure 2a)) was the first ruthenium based complex to reach human clinical investigations. In preclinical investigations in several tumor animal models, exhibited inhibition of tumor metastases and appeared to lack cytotoxic actions. It succeeded in phase I clinical studies, but in phase II clinical studies showed only limited efficacy which prevented further clinical development of NAMI-A [11]. Another ruthenium therapeutic, indazolium *trans*-tetrachloridobis(1*H*-indazole)ruthenate(III)] (KP1019) (Figure 2b)) entered phase I clinical trials. Its low solubility limited its further development [12], but in its place, a more soluble sodium salt, KP1339 (Figure 2), is currently undergoing clinical trials [13]. These Ru (III) complexes are believed to be activated in vivo through reduction to Ru(II). The Ru (II)

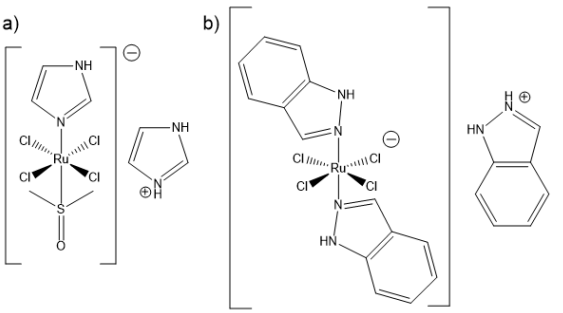

Figure 2: a) NAMI-A, trans-[tetrachlorido(DMSO)(imidazole)ruthenate(III)]; b) KP1019, trans-tetrachloridobis(1H-indazole)ruthenate(III)].

complexes formed upon reduction retain an octahedral structure and can bind to DNA and proteins [14].

Also, many organometallic Ru (II) complexes have been designed and developed as anticancer drugs with potent therapeutic properties. Half-sandwich metal complexes are among the most widely investigated metal-based anticancer drug candidates and feature a π-bound ligand (Ar), often an arene or a cyclopentadienyl (Cp) derivative such as η^5-pentamethylcyclopentadienyl (Cp*), namely "piano-stool". The most prominent representatives are the RAPTA complexes with a monodentate-coordinated 1,3,5-triaza-7-phosphaadamantane (PTA) and the RAED compounds with a bidentate 1,2-diaminoethane ligand (Figure 3) [15]. Ru (II)–arene species bearing ethylenediamine ligands (Figure 3, b)) seem to target DNA and exhibit potent activity in vitro and against in vivo models [14]. Like the cisplatin, they hydrolyse and bind to DNA, but monofunctionally as they have only one labile monodentate ligand [9][14]. In general, metal complexes bind to DNA by both covalent and non-covalent interactions. Covalent binding involves the coordination of the nitrogenous base or the phosphate moiety of the DNA to the central metal ion and is possible in complexes where the metal is coordinatively unsaturated or is coordinated to substitutionally labile ligands. The three different non-covalent binding modes are intercalation, which involves the stacking of the molecule between the base pairs of DNA, groove binding which comprises the insertion of the molecule into the major or minor grooves of DNA, and the electrostatic binding (Figure 4).

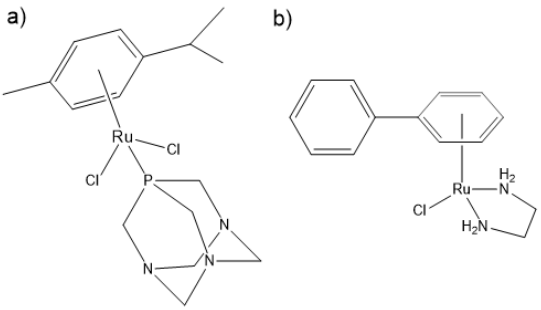

Figure 3: Some organometallic Ru (II) complexes with antitumoral properties, (a) [Ru (p-cymene)Cl_2(PTA)], (b) RAED, [Ru(η^6-1,1'-biphenyl) (en)Cl].

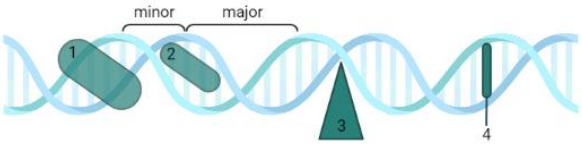

Figure 4: Non-covalent interaction modes. (1) major groove, (2) minor groove, (3) electrostatic and (4) intercalation.

Many Ruthenium compounds have modes of action that involve interactions with proteins rather than DNA and with enzymes, genes, and lipids, having a significant role in tumor growth, survival, and metabolism. They can exhibit anticancer activity via activation of a wide range of cellular pathways (Figure 5), offering the means to reinforce many cell-death mechanisms. Activation of intrinsic and extrinsic pathways in cells leads to primarily induction of apoptosis (programmed cell death). The intrinsic pathway, also known as the mitochondria-mediated pathway, is promoted by DNA damage, oxidative stress, and endoplasmic reticulum (ER) stress [11][16].

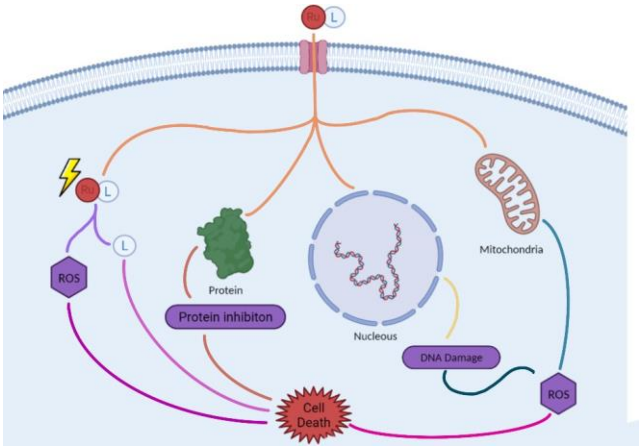

Figure 5: Different targets of ruthenium complexes.

Among the new ruthenium (II) compounds investigated, coordinatively saturated, inert Ru (II) polypyridyl complexes are receiving increasing attention due to their rich physiochemical and biological properties, ability to form diverse rigid geometries, tuneable Ru (II)/(III) redox states under physiological conditions for activation by reduction and tuneable ligand substitution kinetics [17]. Moreover, the application of Ru (II) complexes as effective photosensitizers in photodynamic

therapy (PDT) and photoactivated chemotherapy (PACT) provide spatiotemporal control over conventional chemotherapy [18][19].

Photodynamic therapy (PDT) uses a drug that is activated by light, called a photosensitizer or photosensitizing agent (PS), to kill cancer cells. The light can come from a laser or other source, such as LEDs. The absorption of a photon for the PS agent promotes an electron from the singlet ground state to a singlet excited state which can decay non-radiatively via intersystem crossing to a low-lying triplet state. From this state, an electron can be transferred to biological substrates to form radicals that react with oxygen to generate ROS, causing oxidative stress, and leading to cell death (type I). There can also be direct energy transfer from the PS excited triplet state to ground state triplet oxygen ($^3O_2$) to generate highly reactive singlet oxygen ($^1O_2$) (type II) (Figure 6). The advantage of this technique is its low systemic toxicity since the PS exerts its activity only where and when the light is irradiated. In the treatment of cancers, the ROS and/or radicals form damage and close blood vessels, cutting off the supply of nutrients to the tumor [20]. In addition, it was demonstrated that PDT may elicit an immune response [18]. One of these ruthenium-based PSs, namely TLD-1433 (Figure 7), is in phase II clinical trial as a PDT PS against bladder cancer [18].

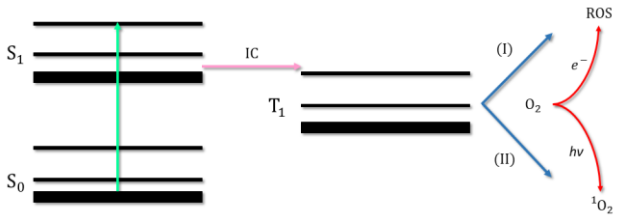

Figure 6: Mechanism of Photodynamic therapy.

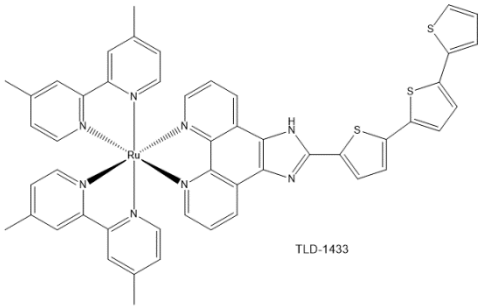

Figure 7: Molecular structure of the ruthenium complex photosensitiser [Ru(dmb)$_2$(IP-3T)]Cl$_2$ (TLD1433).

In contrast, photoactivated chemotherapy (PACT) strategy involves various photochemical processes including ligand dissociation, followed by covalent binding, photo-crosslinking with DNA or electron transfer to DNA through photo-generated active species and ultimately cell death [21].

The compound 2,2':6',2''-terpyridine (trp) and their derivatives are chelating ligands suitable for the formation of transition metal complexes. This is because they have three aromatic pyridine rings linked together via three single bonds that have three nitrogen atoms capable to chelate a wide range of transition metal and lanthanide ions as tridentate ligands [22]. Ruthenium (II) complexes with terpyridine derivatives play an important role in the field of macromolecular chemistry, photochemistry, supramolecular chemistry, nanoscience, photo-physics and catalysis [23]. Differing from the Ru (II) complexes with tris-diimine ligands, $[Ru(diimine)_3]^{2+}$, the complexes with trp have the advantages of avoiding formation of isomers, which may reduce the synthetic challenges for developing new Ru (II) complexes. This kind of compounds also exhibits relatively strong metal-to-ligand charge transfer (^{1}MLCT) absorption in the visible spectral regions (450−600 nm) [24][25]. The functionalization of trp at the 4'- position with different organic moieties allows extend the conjugation of the directly linked aromatic ring.

4. OBJECTIVES

The aim of this project is the preparation and characterization of 4´-substituted ruthenium terpyridine compounds, their photochemical behaviour and study their interaction with DNA.

The specific objectives are:

- The synthesis and characterization of 4'-substituted-2,2':6',2''-terpyridine derived ligands.
- The synthesis and characterization of the ruthenium (III) complexes, [Ru(Rtrp)Cl_3] with these ligands.
- The synthesis and characterization of the ruthenium (II) complexes, [Ru(Rtrp)(*N,N*)Cl]Cl where *N,N*= bipy, phen, dpa.
- The reaction of these compounds with pyridine to prepare [Ru(Rtrp)(*N,N*)(Py)]$(PF_6)_2$.
- Study of their absorption, emission, and excitation spectra and the interaction with DNA by electrophoresis and UV-vis.

5. RESULTS AND DISCUSSION

5.1. SYNTHESIS AND CHARACTERIZATION OF 4'-SUBSTITUTED-2,2':6',2"-TERPYRIDINE LIGANDS.

The general method used for the synthesis of 4'-derivatives of 2,2'-6',2"-terpyridine ligands is represented in (Figure 8) [25]:

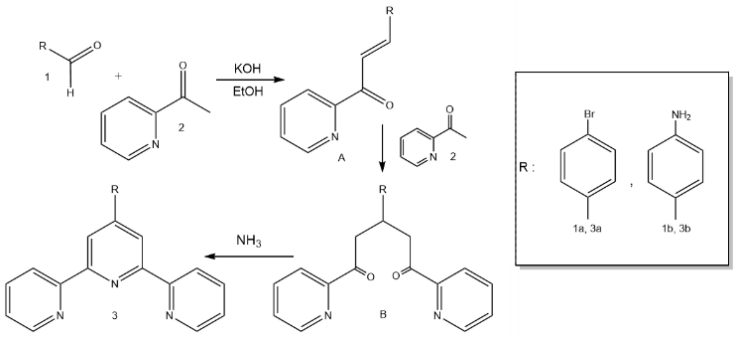

*Figure 8: Synthesis of Rtrp ligand. Brtrp (**3a**) and Anitrp (**3b**).*

The synthesis starts whit a Kröhnke condensation, where the aldehydes 4-bromobenzaldehyde **(1a)** or 4-aminobenzaldehyde **(1b)** are deprotonated and condensed with the 2-acetylpyridine **(2)**. This reaction forms the specie A, a chalcone. The second step is a Michael addition of a second molecule of 2-acetylpyridine forming the 1,5-dione (B). Finally, the cyclization is produced with ammonia to form the central pyridine ring. For practical purification reasons, the stoichiometry aldehyde:2-acetilpyridine of the reaction has been changed from 1:2 to 1:1,7 as acetylpyridine is a viscous liquid that is difficult to eliminate. The new 4'-substituted-

2,2':6',2"-terpyridine derivatives prepared are 4'-(4-bromophenyl)-2,2':6',2"-terpyridine (Brtrp, **3a**) and 4'-(4-aminophenyl)-2,2':6',2"-terpyridine (Anitrp, **3b**).

The ligands 4'-(naphthalen-2-ylmethoxy)-2,2':6',2"-terpyridine (Ntrp**,** **3c**) and 4'-(4-(naphthalen-2-ylmethoxy)phenyl)-2,2':6',2"-terpyridine (BrNtrp, **3d**) were obtained by the reaction of nucleophilic aromatic substitution (S_{NA}) of the chlorine (in 4'-chloro-2,2':6',2"-terpyridine) [26] or the bromine (in **3a**) for naphtalen-2-ylmethanol (Figure 9).

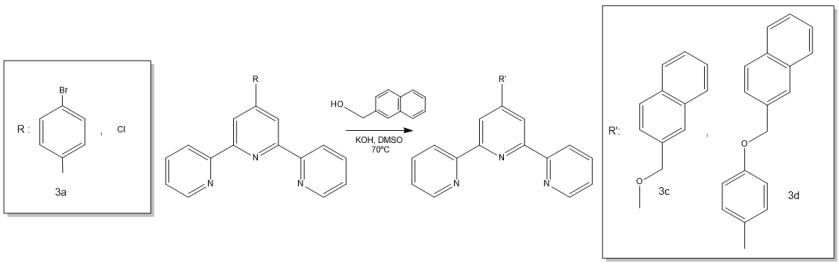

Figure 9: Synthesis of R'trp ligands: Ntrp ***(3c)*** *and BrNtrp* ***(3d)****.*

The ligands were characterized by IR, mass spectrometry and mono- and two-dimensional NMR spectroscopies (see experimental section). The IR spectra of ligands show the characteristic bands of the terpyridine part between 1580-1616 cm^{-1} due to the ν(C=N) group. Furthermore, it can be seen the stretching bands of the substituent group NH_2 at 3300-3500 cm^{-1} for **3b**. The absence of bands around 1715 cm^{-1} in all the ligands spectra indicates that no carbonyls of the 2-acetylpyridine are present.

One- and two-dimensional NMR experiments agree with the structure proposed for each ligand. The common feature of the ^{1}H-NMR spectra is a signal which appears as a singlet in the range 8,0-9,0 ppm and is indicative that the terpyridine group of the ligand has been formed. For **(3c)** and **(3d),** another characteristic peak is the singlet about 5,5 ppm {5,58 ppm **(3c)** and 5,74 ppm **(3d)**} corresponding to the methylene group.

The ligands **(3a)**, **(3b),** and **(3c)** had been synthesized previously in the research group but their synthesis was repeated in order to have product to obtain their ruthenium complexes and study the DNA interaction.

5.2. SYNTHESIS AND CHARACTERIZATION OF RU (III) COMPLEXES.

The reaction of the prepared ligands with $[RuCl_3]\cdot 3H_2O$ allows the obtention of complexes $[Ru(Rtrp)Cl_3]$ (**4**) (Figure 10) [27]:

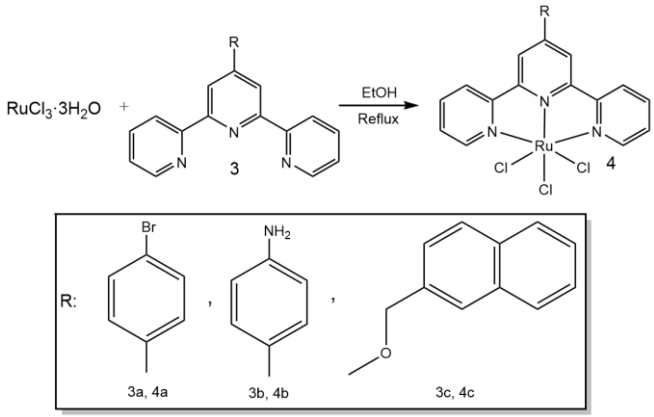

Figure 10: Synthesis of ruthenium (III) complexes [Ru(Rtrp)Cl₃].

Due to their paramagnetic properties these ruthenium (III) complexes have been characterized only by IR and MS. The mass spectra confirm that $[Ru(Brtrp)Cl_3]$ **(4a)**, $[Ru(Anitrp)Cl_3]$ **(4b)** and $[Ru(Ntrp)Cl_3]$ **(4c)** are obtained. The $[Ru(BrNtrp)Cl_3]$ **(4d)** was obtained but the mass spectrum was inconclusive because $[Ru(BrNtrp)Cl_2]^+$ fragment was not observed.

5.3. SYNTHESIS AND CHARACTERIZATION OF RUTHENIUM (II) COMPLEXES.

Treatment of the neutral Ru(III) precursors, $[Ru(Rtrp)Cl_3]$ **(4)** with a neutral (*N,N*) chelating ligand, such a 2,2'-bipyridine (bipy), 1,10-phenantroline (phen) or 2,2'-dipyridilamine *(dpa)*, in presence of trimethylamine (Et_3N) as reductor agent and excess de LiCl afforded the Ru(II) complexes $[Ru(Rtrp)(N,N)Cl]Cl$ (**5**) where Rtrp = **3a** and *N,N* = bipy, phen and dpa and Rtrp = **3c** and *N,N* = bipy (Figure 11) [27]. These monofunctional compounds could be interesting because, in addition to their photophysical properties, they could interact with DNA via intercalation or/and covalent binding.

All the compounds prepared: [Ru(Brtrp)(*N,N*)Cl]Cl where *N,N* = bipy (**5a**), phen (**5a'**) and dpa (**5a"**) and [Ru(Ntrp)(bipy)Cl]Cl **(5c),** were characterized by IR, mass spectrometry and mono- and two-dimensional NMR spectroscopies (see Experimental Section and Appendix)). Its characterization data agreed with the structures proposed.

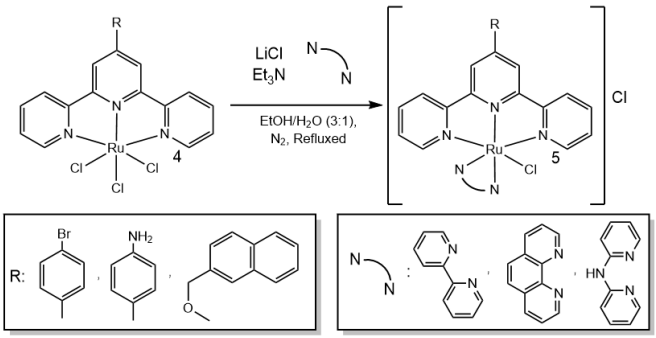

*Figure 11: Synthesis of ruthenium (II) complexes [Ru(Rtrp)(N,N)Cl]Cl (**5**).*

In the ^{1}H NMR spectra of the compounds [Ru(Brtrp)(*N,N*)Cl]Cl there are seven aromatic resonances assigned to the symmetric Brtrp ligand placed in the equatorial plane and eight peaks assigned to the two inequivalent halves of the bidentate ligands perpendiculars. The protons of the halve over the Brtrp plane are closer to the axial chloride therefore they appear in the ^{1}H NMR spectrum shifted downfield compared to the proton peaks corresponding on the other ring. It is worth noting that the most characteristic peak of ^{1}H NMR spectrum of these compounds is the doubled assigned to H^a ($\delta_H{}^a$ **(5a)** = 10,23; $\delta_H{}^a$ **(5a')** = 10,45 and $\delta_H{}^a$ **(5a")** = 9,43 ppm). When the bidentate (*N,N*) ligand is dpa, compound **(5a")**, it can be observed also the resonance assigned to the proton of the NH group ($\delta_H{}^k$ **(5a")** = 10,61 ppm, (Figure 12)).

The ^{1}H NMR spectrum of the compound [Ru(Ntrp)(bipy)Cl]Cl shows the aromatic resonances assigned to the Ntrp ligand. This ligand has also two methylenic protons that appear as a singlet upfield ($\delta_H{}^{10}$ **(5c)** = 5,74 ppm, see Experimental Section). The resonance of the H^a of the bipy ring next to chloride is a doublet at δ = 10,07 ppm.

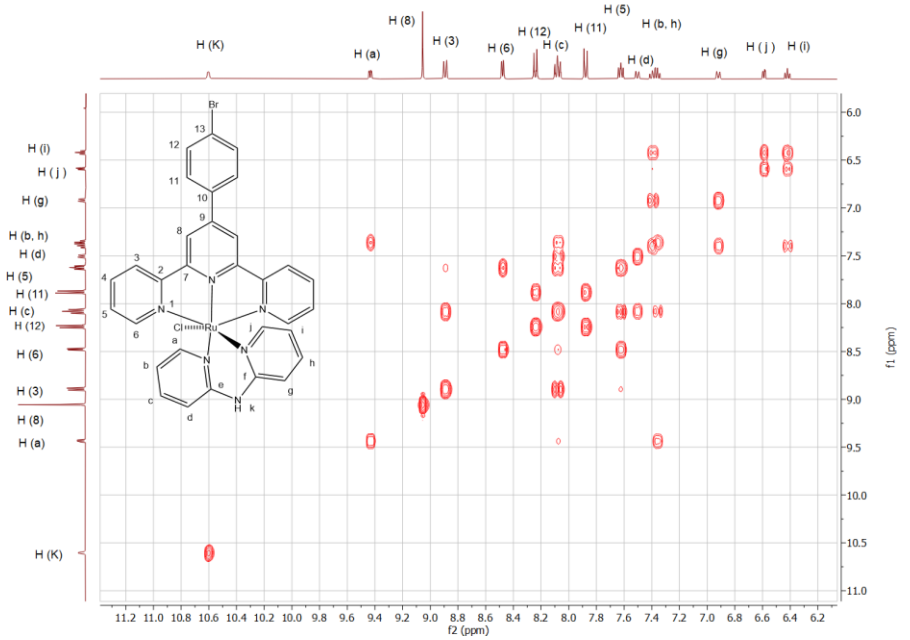

*Figure 12: Bidimensional RMN {^{1}H-^{1}H} COSY spectrum of (**5a"**) in DMSO-d^6*

The IR spectra of all the complexes [Ru(Rtrp)(*N,N*)Cl]Cl show the typical bands of the trp ligands: the aromatic C-H stretching in the 3060-2850 cm^{-1} region, and the characteristic strong band at 1395-1616 cm^{-1} zone assigned to ν(C=N) and ν(C=C).

The reaction of [Ru(Anitrp)Cl$_3$] **(4b)** with bipy or phen produces the desired products **(5b)** and **(5b')**, respectively, but impurified with [Ru(*N,N*)$_3$]Cl$_2$ where *N,N* = bipy in the case of **(5b)** or phen for **(5b')** and was not possible to separated.

Sadler and co-workers [28] demonstrated that irradiation of inert half-sandwich Ru(II) compounds of the type [(η^6-arene)Ru(*N,N'*)(L)]$^{2+}$ (where *N,N'* is a nitrogen chelating ligand, and L is a nitrogen monodentate ligand such as pyridine) with visible light leads to the selective dissociation of monodentate ligand (i.e. activation). In order to prepare similar compounds with Brtrp, *N,N* bidentate ligands and pyridine, the reaction of the chloride complexes **(5a)**, **(5a')** and **(5a")** with pyridine was carried out as reported in [29] (Figure 13). In a first step, the chloride complexes reacted with $AgNO_3$ to afford the aqua adducts [Ru(Brtrp)(*N,N*)(H_2O)]$^{2+}$ which were then treated with an excess of pyridine to give [Ru(Brtrp)(*N,N*)(py)](PF_6)$_2$ **(6)** where *N,N* = bipy **(6a)**, phen **(6a')** and dpa **(6a")** after precipitation with NH_4PF_6.

The characterization of these compounds by mass spectrometry, IR, and ^{1}H NMR spectroscopies indicate that the structure of compounds agrees with the formulae proposed for **(6a')** and **(6a")**.

The most characteristic feature in the ^{1}H NMR spectra of these pyridine compounds is the important shift to upfield of the resonance of the H^a of the bidentate ligand when the axial chloride is substituted by a pyridine ring (for instance, δ_{H^a} **(6a")** = 7,81 ppm while δ_{H^a} **(5a")** = 9,43 ppm, see Experimental Section).

The compound $[Ru(Brtrp)(bipy)(py)](PF_6)_2$ **(6a)** was no isolate. The solid precipitate was a mixing of different substances.

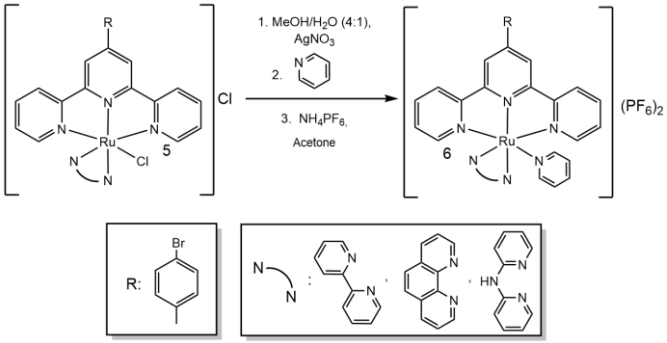

Figure 13: Synthesis of ruthenium (ll) complexes $[Ru(Brtrp)(N,N)(py)](PF_6)_2$ where N,N = bipy ***(6a)****, phen* ***(6a')*** *and dpa* ***(6a")****.*

Also has been possible the synthesis and characterization of symmetrical and unsymmetrical Ru(II) terpyridine complexes $[Ru(Brtrp)_2](PF_6)_2$ **(7a)** and $[Ru(Brtrp)Ntrp](PF_6)_2$ **(7b)**. The method used [30] (Figure 14, 15) consists of a redox reaction with *N*-methylmorpholine as a reducing agent in methanol, under nitrogen atmosphere. The ruthenium (II) complex was precipitated from the resulting dark brown solution by the addition of an excess of ammonium hexafluorophosphate.

The characterization data agrees with the structure proposed for both compounds (see Experimental Section).

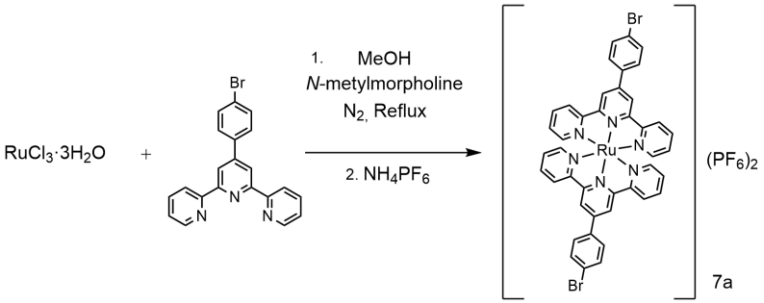

*Figure 14: Synthesis of [Ru(Brtrp)$_2$](PF$_6$)$_2$ (**7a**).*

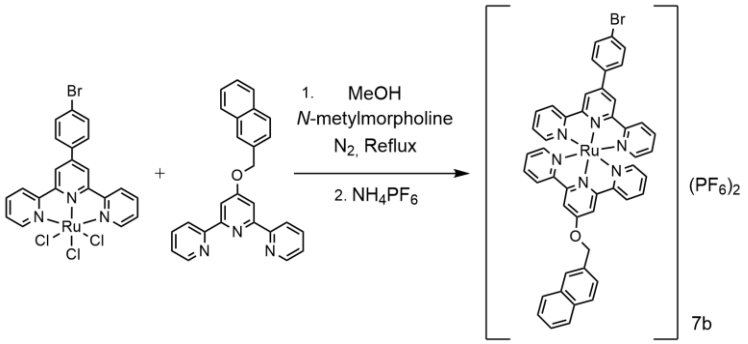

*Figure 15: Synthesis of [Ru(Brtrp)(Ntrp)](PF$_6$)$_2$ (**7b**).*

5.4. UV-VIS AND FLUORESCENCE STUDIES OF THE RUTHENIUM (II) COMPLEXES.

The UV-Vis and fluorescence spectra have been recorded. The application of the Lambert-Beer's law (equation 1) allows to obtain the extinction coefficient (appendix 4, table 1).

$$A = l \cdot c \cdot \varepsilon$$

Equation 1: Lambert-Beer law.

The wavelength of the maximum of the MLCT band (*ca.* 500 nm) usually does not show significant differences with the band of the excitation spectrum (Figure 16a)). It is interesting to note that in the case of [Ru(Ntrp)(bipy)Cl]Cl (**5c**) (Figure 16b)) there are differences between in the wavelength of both maximums that can be explained by the formation of excimers [31].

The emission and excitation spectra are used to evaluate the fluorescent properties of the complexes, as well as to indicate which has the highest quantum yield. The higher emission intensity indicate that the derivative dpa compounds (**5a''**) and (**6a''**) have the better quantum yield.

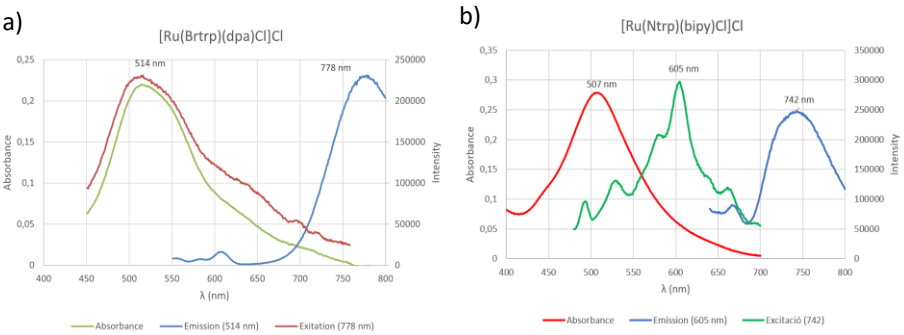

*Figure 16: UV-Vis and fluorescence spectra: a) (**5a''**) and b) (**5c**), 25μM in acetonitrile.*

5.5. UV-VIS STUDIES OF DNA-RUTHENIUM COMPLEX (II) INTERACTION.

The interaction of the complexes **(5a)** and **(7a)** with DNA was studied by UV-Vis spectroscopy. All the experiments were done by an addition of increasing amounts of DNA, from 0 to 100 μM, (in base pairs) to a solution of 25 μM of the complex, in a cacodylate/NaCl buffer. The samples were incubated for 1 hour at 37ºC (Figure 17a)). To compare the DNA interaction with the metallic complexes, the K_b (intrinsic binding constant) was calculated, using equation 2, where ε_a is the apparent extinction coefficient of the complex (A_{obs}/[complex]), ε_f is the extinction coefficient of the free complex in the solution and ε_0 is the extinction coefficient of the complex in the fully DNA bound form.

$$\frac{[DNA]}{(\varepsilon_a - \varepsilon_f)} = \frac{[DNA]}{(\varepsilon_0 - \varepsilon_f)} - \frac{1}{K_b(\varepsilon_0 - \varepsilon_f)}$$

Equation 2.

The constant K_b, was determined from the corresponding plot of [DNA]/(ε_a- ε_f) vs. [DNA] (Figure 17b)).

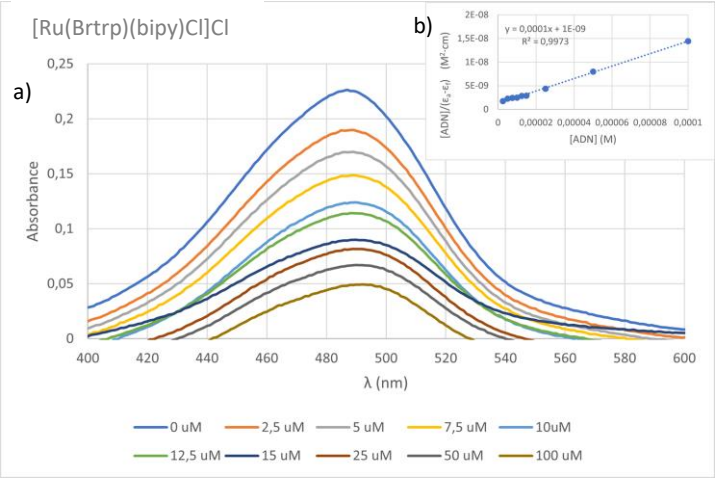

*Figure 17: a) UV-Vis spectra of (**5a**) and b) [DNA]]/(εa- εf) vs. [DNA].*

For the complexes have been obtained a moderately strong intrinsic binding constants (K_b = 1,11·10^5 M^{-1} for **(5a)** and K_b = 3,59·10^5 M^{-1} for **(7a)**), compared to similar complexes [26].

The bathochromic shift together the hypochromic effect of the absorption band observed in both complexes **5a** and **7a** indicate a covalent and intercalation interaction between the complexes and DNA [30].

5.6. ELECTROPHORESIS STUDIES OF DNA-RUTHENIUM COMPLEX INTERACTION.

The interaction of the Ruthenium complexes with DNA can be visualized by electrophoresis gel of agarose. This technique is one of the most used to separate and identify DNA fragments. Pure plasmid DNA gives two bands, the intense one corresponding to supercoiled DNA (Form I), while the second one is ascribed to circular nicked form (Form II). There is another form which is linear (Form III) and migrates between Form II and Form I.

All the samples were prepared for duplicate in a solution of cacodylate/NaCl buffer with 2% of DMSO and incubated at 37 ºC for half an hour with pBR322 plasmid DNA 15 μM in base pairs. Then, one of the duplicate is irradiated (even-numbered samples in Figures 18-20) with white light (which contains the maximum absorbance wavelength of the complex).

Next, the samples were quenched with 4 μL of loading buffer (5 mM xylene cyanol and 30% glycerol) and electrophoresed on agarose gel in TBE buffer (Tris-borate-EDTA) for 1 h

at 100 V. The gel was placed in 150 mL of the buffer of TBE and 15 µL of SYBR Safe, a display buffer and was agitated overnight. (Figure 18, 19 and 20).

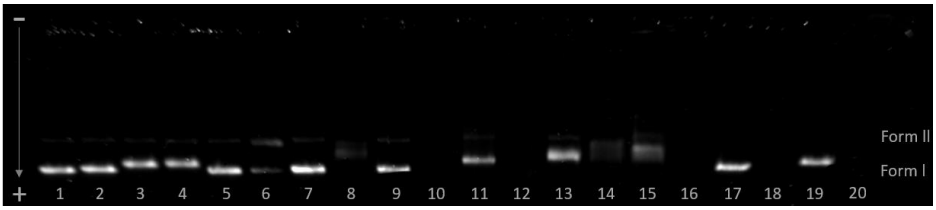

*Figure 18: Agarose gel electrophoresis of pBR322 plasmid DNA. Lane 1, 2: DNA control; 3, 4: cisplatin (10µM); 5, 6 [Ru(phen)$_3$]Cl$_2$ (10µM); 7, 8: (**4a**) (10µM); 9, 10: (**5a**) (10µM); 11, 12: (**5a**) (50µM);); 13, 14: (**5a'**) (10µM); 15, 16: (**5a'**) (50µM); 17, 18: (**5a"**) (10µM); 19, 20: (**5a"**) (50µM). The rate of the [complex]/[DNA] were 0,67 for [complex] of 10 µM and 3,33 for [complex] of 50 µM.*

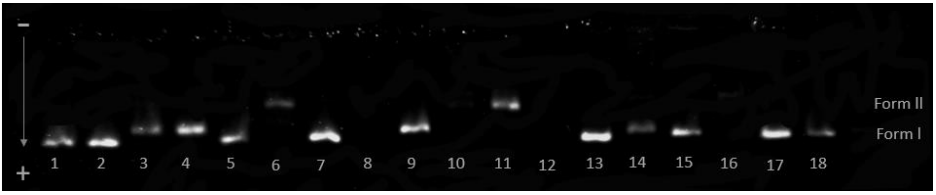

*Figure 19: Agarose gel electrophoresis, of pBR322 plasmid DNA. Lane 1, 2: DNA control; 3, 4: cisplatin (10µM); 5, 6 [Ru(phen)$_3$]Cl$_2$ (10µM); 7, 8: (**6a**) (10µM); 9, 10: (**6a**) (50µM); 11, 12: (**6a'**) (50µM); 13, 14: (**6a'**) (10µM); 15, 16: (**6a"**) (10µM); 17, 18: (**6a"**) (50µM). The rate of the [complex]/[DNA] were 0,67 for [complex] of 10 µM and 3,33 for [complex] of 50 µM.*

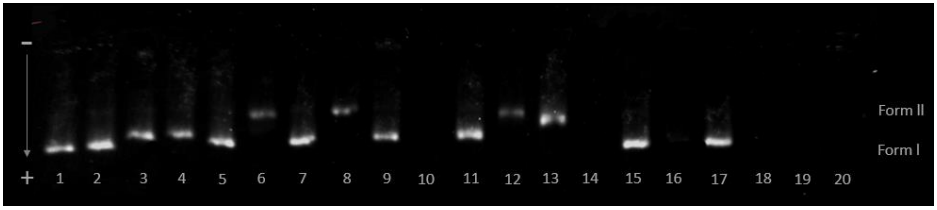

*Figure 20: Agarose gel electrophoresis of pBR322 plasmid DNA. Lane 1, 2: DNA control; 3, 4: cisplatin (10µM); 5, 6 [Ru(phen)$_3$]Cl$_2$ (10µM); 7, 8: (**4c**) (10µM); 9, 10: (**5c**) (10µM); 11, 12: (**5c**) (50µM);); 13, 14: (**7a**) (10µM); 15, 16: (**7a**) (50µM); 17, 18: (**7b**) (10µM); 19, 20: (**7b**) (50µM). The rate of the [complex]/[DNA] were 0,67 for [complex] of 10 µM and 3,33 for [complex] o 50 µM.*

The results of the three gels give information of two effects, the interaction between the complex and the DNA in the non-irradiated samples and the effect of irradiating the samples.

It can be observed that cisplatin has no photosensitising effect and does not cause any change compared to the non-irradiated sample. In contrast, ruthenium complexes in general leads to DNA fragmentation. This effect increases when the concentration is bigger, as expected. If the interaction between the complex and the DNA is between the major or minor groove, or electrostatic, there is no delay in DNA mobility. On the other hand, if the interaction is covalent or if there is intercalation between the DNA bases, a delay in the mobility appears, produced by the modification of the DNA structure. As expected, cisplatin produces a delay in mobility, due to the covalent interaction. $[Ru(phen)_3]Cl_2$ does not produce changes in mobility, because its interaction is established to be in the grooves. At 10 μM, not all the complexes synthesized cause obvious changes in mobility, but at 50 μM, the change is evident. In contrast, complexes **(7a)** and **(7b)** have no labile ligands to release. They intercalate into the DNA, which produces the delay.

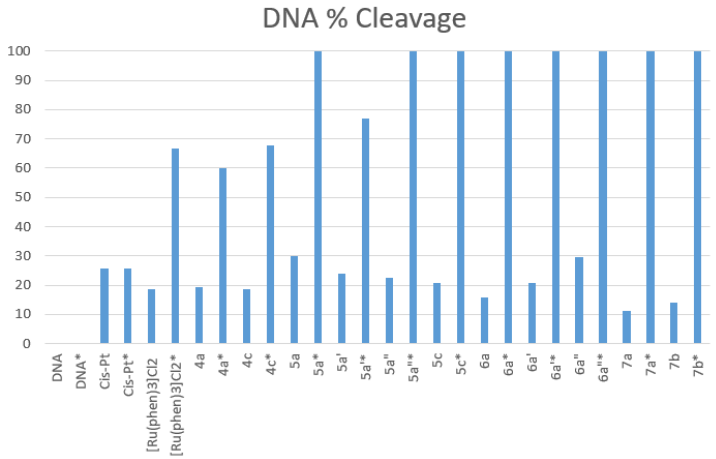

*Figure 21: DNA % cleavage representation. [Complex]= 10 μM. (**4a**) non-irradiated sample, (**4a***) irradiated sample.*

The intensity data provide information on the % of DNA that has been cleaved. In the previous graph (Figure 21), this percentage is plotted for each complex. The non-irradiated

samples show a low cleavage, less than 30%. The photosensitising effect has a positive character in the irradiated samples, increasing the fragmentation. The complexes **(4a)**, **(4c)** and **(5a')** have not completely cleaved the DNA, but their results are favourable, with an excision of more than 60%. The other complexes have a cleavage of 100%.

9. EXPERIMENTAL SECTION.

9.1. MATERIALS AND METHODS

The solvents and reagents used in this project were obtained from commercial sources and used without further purification.

Routine NMR spectra were obtained with a Mercury 400 MHz instrument. Mono-1H, 13C{1H} and bidimensional ({1H-1H}-COSY and {1H-13C}-HSCQ) NMR experiments were recorded with a Bruker Avance DMX 500 MHz instrument at 298 K. FT-IR Thermo Nicolet 330, in a 4000-400 cm-1 range. UV-Vis was performed with a Varian Cary-100 spectrophotometer. The Fluorescence spectra were made with Nanolog-Horiba Jobin Yvon. The instrument used for the agarose electrophoresis images was the Gel Doc EZ Imager.

9.2. PREPARATION OF LIGANDS:

9.2.1. General method for the synthesis of 4'-substituted-2,2':6',2"-terpyridine 3a and 3b [25]:

2-Acetylpyridine and KOH were added to a solution of the aldehyde in EtOH. The resulting mixture was left to react for 5 min and then a solution of NH_3 (25%) was added. This solution was heated reflux for 5 h. The precipitate was collected by filtration and washed with EtOH.

9.2.1.1 Synthesis of 4'-(4-bromophenyl)-2,2':6',2"-terypiridine (3a):

4-bromobenzaldehyde (2,47 g, 13,34 mmol) in EtOH (35 mL), 2-acetylpyridine (2.5 mL, 22.27 mmol), KOH (0,75 g, 13.34 mmol) and NH_3 (15 mL, 25%).

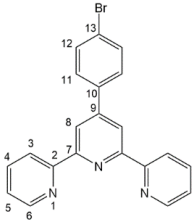

White solid. Yield: 1,957g (37,9 %). IR (KBr): 3375, 3057, 2912, 1583, 1490 cm^{-1}. ^1H NMR ($CDCl_3$, 500 MHz, ppm): δ 8,73 (dd, J = 5,0; 2,7 Hz, 2H, H^3), 8,70 (s, 2H, H^8), 8,67 (dd, J =8,7; 1,1 Hz, 2H, H^6), 7,88 (td, J =7,6; 2,4 Hz, 2H, H^4), 7,78 (dd, J = 8,4; 2,1 Hz, 2H, H^{12}), 7,64 (dd, J = 8,4; 2,9 Hz, 2H, H^{11}), 7,36 (td, J = 5,9; 0,8 Hz, 2H, H^5). ^{13}C NMR ($CDCl_3$, 125,7 MHz, ppm): δ 156,3(C^7), 156,2(C^2), 149,3(C^6), 149,2(C^9), 137,6(C^{10}), 137,1(C^4), 132,3(C^{11}), 129,0(C^{12}), 124,1(C^5), 123,6(C^{13}), 121,5(C^3), 118,7(C^8). HRMS (ESI): m/z = 388,04 (M^+).

9.2.1.2. Synthesis of 4'-(4-aminophenyl)-2,2':6',2"-terpyridine (3b):

4-aminobenzaldehyde (0,5 g, 4,13 mmol) in EtOH (8 mL), 2-acetylpyridine (0.78 mL, 6,95 mmol), KOH (0,23 g, 4,13 mmol) and NH_3 (4,7 mL, 25%).

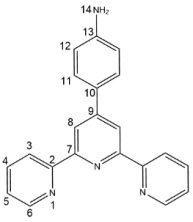

Dark yellow solid. Yield: 0,547g (40,9 %). IR (KBr): 3474, 3385, 1614, 1583, 1521, 791 cm^{-1}. ^1H NMR (DMSO-d_6, 500 MHz, ppm): δ 8,74 (ddd, J = 4,8; 1,8; 0,8 Hz, 2H, H^3), δ 8,64 (dd, J= 8,0; 1,1 Hz, 2H, H^6), δ 8,62 (s, 2H, H^8), δ 8,01 (td, J =7,8; 1,7 Hz, 2H, H^4), δ 7,66 (d, J = 8,4 Hz, 2H, H^{11}), δ 7,51 (dd, J = 7,5; 4,7Hz, 2H, H^5), δ 6,72 (d, J = 8,6 Hz, 2H, H^{12}), δ 5,60 (s, 2H, H^{14}). ^{13}C NMR (DMSO-d_6, 125,7 MHz, ppm): δ 155,0(C^7), 155,0(C^2), 150,2(C^9), 149,3(C^{13}), 149,0(C^3), 137,0(C^4), 127,3(C^{11}), 124,0(C^5), 123,4(C^{10}), 120,5(C^6), 115,9(C^8), 114,8(C^{12}). HRMS (ESI): m/z = 325,11 (M^+)

9.2.2. General method for synthesis of 4'-substituted-2,2':6',2"-terpyridine 3c and 3d [26]:

An amount of 2-naphthalenemethanol was added to a suspension of KOH in 15 mL of DMSO. After stirring for 30 minutes at 70 °C, the stoichiometric quantity of Cltrp (for **3c**) or Brtrp (for **3d**) was added, and the resulting reaction mixture was further stirred for 4 hours at 70 °C. Subsequently, this reaction mixture was poured into 100 mL of ice water. The precipitate formed was filtered off, washed with cold water and dried under reduced pressure.

9.2.2.1. Synthesis of 4'-(naphthalen-2-ylmethoxy)-2,2':6',2"-terpyridine (3c):

2-naphtalenemethanol (0,158 g, 1 mmol), KOH (0,280 g, 5 mmol), DMSO (2,5 mL), 4-chloro-2,2':6',2"-terpyridine (0,268 g, 1mmol).

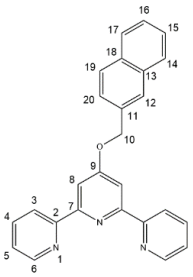

Off-white solid: Yield: 0,129g (33,4%). IR (KBr): 3412, 3047, 3007, 2949, 2918, 1574, 1552, 1347 cm^{-1}. ^1H NMR (DMSO-d_6, 500 MHz, ppm): δ 8,72 (dd, J = 4,7; 1,9 Hz, 2H, H^3), 8,63 (dd, J = 8,1; 1,2 Hz, 2H, H^6), 8,13 (s, 2H, H^8), 8,08 (s, 1H, H^{12}), 8,01 (td, J = 7,6; 1,8 Hz, 2H, H^4), 7,99 (1H, H^{19}), 7,75 (1H, H^{20}), 7,67 (1H, H^{17}), 7,54 (2H, H^5), 7,52 (1H, H^{14}), 7,51 (1H, H^{15}), 7,49 (1H, H^{16}), 5,58 (s, 2H, H^{10}). ^{13}C NMR (DMSO-d_6, 125,7 MHz, ppm): δ 166,2(C^9), 156,8(C^7), 154,8(C^2), 149,3(C^3), 137,4(C^4), 133,9(C^{11}), 133,0(C^{14}), 132,8(C^{13}), 132,6(C^{18}), 128,1(C^{19}), 127,9(C^{20}), 127,7(C^{15}), 126,4(C^{12}), 126,2(C^5), 125,5(C^{17}), 124,6(C^{16}), 120,9(C^6), 107,2(C^8), 69,6(C^{10}). HRMS (ESI): m/z = 390,23 (M + H^+), 141,07 [(2-methyl)naphthalene-H]$^+$.

9.2.2.1. Synthesis of 4'-((naphthalen-2-ylmethoxy)phenyl)-2,2':6',2"-terpyridine (3d):

2-naphtalenemethanol (0051 g, 0,32 mmol), KOH (0,089 g, 1,61 mmol), DMSO (2,5 mL), 4'-(4-bromophenyl)-2,2':6', 2"-terypiridine (**3a**) (0,125 g, 0,32mmol).

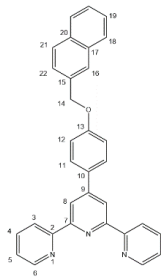

Off-white solid: Yield: 0,120 g (80,5 %). IR (KBr): 3385, 3056, 1579, 1494, 1467, 1383 cm^{-1}. ^1H NMR (DMSO-d_6, 500 MHz, ppm): δ 8,75 (d, J = 4,8 Hz, H^3), 8,70 (s, H^8), 8,67 (d, J = 7,9 Hz, H^6), 8,04 (td, J = 7,6; 1,8 Hz, H^4), 7,97 - 7,92 (m, H^{21}, H^{22}), 7,90 (d, J = 8,8 Hz, H^{11}), 7,80 - 7,75 (m, H^{12}, H^{18}), 7,68 (s, H^{16}), 7,58 – 7,52 (m, H^5, H^{19}), 5,74 (s, H^{14}). HRMS (ESI): m/z = 466,66 ($M + H^+$), 387,87 Ntrp + H]$^+$.

9.3. PREPARATION OF RUTHENIUM COMPLEXES:

9.3.1. General procedure for the synthesis Ru(III) complexes [Ru(Rtrp)Cl_3] (4) [27]:

An amount of $RuCl_3 \cdot 3H_2O$ was dissolved in EtOH and the resulting brown solution was refluxed until the colour of the solution changed to green (ca. 2 h). Then the stoichiometric amount of 4'-substituted-2,2':6':2"-terpyridine was added and reflux continued for 5 hours. The precipitate formed by cooling the solution to room temperature was filtered and washed with ethanol.

9.3.1.1. Synthesis of [Ru(Brtrp)Cl_3] (4a):

$RuCl_3 \cdot 3H_2O$ (0,180 g, 0,688 mmol), EtOH (40 mL), 4'-(4-bromophenyl)-2,2':6',2"-terypiridine **(3a)** (0,267 g, 0,688 mmol).

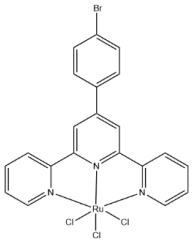

Dark red solid: Yield: 0.360g (88,1%). IR (KBr): 3050, 3012, 1590, 1353, 1004 cm^{-1}. HRMS (ESI): m/z = 560,94 {[Ru(Brtrp)Cl_2]$^+$}, 438,84 {[(Ru(Brtrp)$_2$]$^{2+}$} .

9.3.1.2. Synthesis of [Ru(Anitrp)Cl_3] (4b):

$RuCl_3 \cdot 3H_2O$ (0,180 g, 0,688 mmol), EtOH (40 mL), 4'-(4-aminophenyl)-2,2':6',2"-terpyridine **(3b)** (0,223 g, 0,688 mmol).

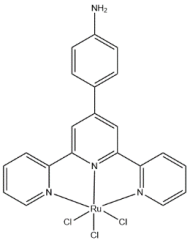

Deep brown solid: Yield: 0,243 g (42,7%). IR (KBr): 3434, 3216, 2349, 1597, 1454, 1392 cm^{-1}. HRMS (ESI): m/z = 496,02 {$[Ru(anitrp)Cl_2]^+$}.

9.3.1.3. Synthesis of $[Ru(Ntrp)Cl_3]$ (4c):

$RuCl_3 \cdot 3H_2O$ (0,180 g, 0,688 mmol), EtOH (40 mL), 4'-(naphthalen-2-ylmethoxy)-2,2':6',2"-terpyridine **(3c)** (0,268 g, 0,688 mmol).

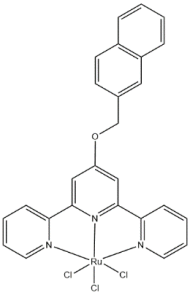

Deep brown solid: Yield: 0,283 g (68,9 %). IR (KBr): 3568, 3047, 1588, 1472, 1410, 1205 cm^{-1}. HRMS (ESI): m/z = 561,03 {$[Ru(Ntrp)Cl_2]^+$}, 440,80 {$[(Ru(Ntrp)_2]^{2+}$}.

9.3.1.4. Synthesis of $[Ru(BrNtrp)Cl_3]$ (4d):

$RuCl_3 \cdot 3H_2O$ (0,100 g, 0,380 mmol), EtOH (20 mL), 4'-((naphthalen-2-ylmethoxy)phenyl)-2,2':6',2"-terpyridine **(3d)** (0,177 g, 0,380 mmol).

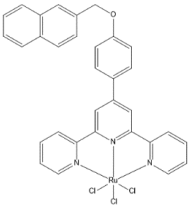

Deep brown solid: Yield: 0,228 g (89,2 %). IR (KBr): 3452, 3065, 1601, 1463, 1241, 996 cm^{-1}. HRMS (ESI): m/z = 438,82 {$[Ru(BrNtrp)(trp+Ph)]^+$}.

9.3.2. General method for the synthesis of Ruthenium(II) complexes, [Ru(Rtrp)(*N,N*)Cl]Cl (5) [27]:

A weighed amount of $[Ru(Rtrp)Cl_3]$ (4) was suspended in an EtOH/H_2O mixture (3:1) containing 10 eq. of LiCl under N_2. After 5 min, 3 eq. of triethylamine and the stoichiometric amount of the chelating ligand were added. The mixture was refluxed under N_2 for 5h. After this time, the solution was filtered while hot to remove any undissolved materials and concentrated to

ca. 1/4 of the initial volume. The storage of the concentrate for 24 hours at 4ºC induces the precipitation of the product. It was collected by filtration.

9.3.2.1. Synthesis of [Ru(Brtrp)(bipy)Cl]Cl (5a):

[Ru(Brtrp)Cl_3] **(4a)** (0.150 g, 0,252 mmol), 2,2'-bipyridine (0,039 g, 0,252mmol), LiCl (0,108 g, 2,52mmol), Et_3N (104 µL, 0,755 mmol), EtOH (22,5 mL), H_2O (7,5 mL).

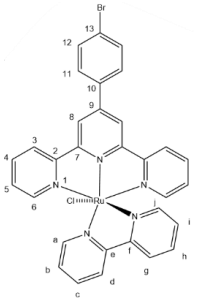

Dark red solid: Yield: 0,095 g (52,4%). IR (KBr): 3417, 1632, 1610, 1459, 1427, 1387 cm^{-1}. ^1H NMR (DMSO-d_6, 500MHz, ppm): δ 10,23 (dd, J = 5,4; 1,6 Hz, 1H, H^a), 8,75 (s, 2H, H^8), 8,62 (dd, J = 8,3; 1,0 Hz, 1H, H^d), 8,54 (dd, J = 8,2; 1,4 Hz, 2H, H^3), 8,32 (dd, J = 8,1; 1,0 Hz, 1H, H^g), 8,27 (dt, J = 7,6; 7,6; 1,8 Hz, 1H, H^c), 8,05 (d, J = 8,6 Hz, 2H, H^{12}), 7,97 (dd, J = 7,1; 5,8 Hz, 1H H^b), 7,90 (td, J = 7,7; 1,6 Hz, 2H, H^4), 7,86 (d, J = 8,6 Hz, 2H, H^{11}), 7,69 (dd, J = 5,5; 1,5 Hz, 2H, H^6), 7,65 (d, J = 1,5 Hz, 1H, H^h) 7,35 (dd, J = 5,7; 1,7 Hz, 1H ,H^i) 7,28 (dd, J = 6,7; 5,4 Hz, 2H, H^5), 6,95 (dd, J = 7,3; 5,7 Hz, 1H, H^i). ^{13}C NMR (DMSO-d_6, 125,7 MHz, ppm): δ 159,7(C^7), 159,1(C^2), 157,1(C^e), 156,6(C^f), 153,4(C^j), 153,3(C^a), 153,0(C^9), 145,7(C^{10}), 138,0(C^4), 137,5(C^c), 136,5($C^{6,h}$), 133,5(C^{12}), 130,5(C^{11}), 128,5(C^5), 128,3(C^b), 127,9(C^{13}), 127,0(C^i), 124,7(C^3), 124,4(C^d), 124,2(C^g), 121,3(C^8). HRMS (ESI): m/z = 682,09 {[Ru(Brtrp)(bipy)Cl]$^+$}.

9.3.2.2. Synthesis of [Ru(Brtrp)(phen)Cl]Cl (5a'):

[Ru(Brtrp)Cl_3] **(4a)** (0.150 g, 0,252 mmol), 1,10-phenantroline (0,036 g, 0,252mmol), LiCl (0,108 g, 2,52mmol), Et_3N (104 µL, 0,755 mmol), EtOH (22,5 mL), H_2O (7,5 mL).

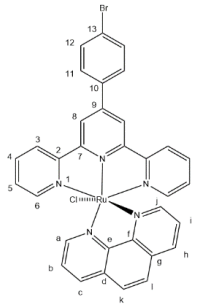

Dark red solid: Yield: 0,137 g (73,5%). IR (KBr): 3421, 3372, 3038, 1605, 1401, 1392, 1080 cm^{-1}. ^1H NMR (DMSO-d_6, 500MHz, ppm): δ 10,45 (dd, J = 5,1; 1,3 Hz, 1H, H^a), 8,82 (dd, J = 8,3; 1,2 Hz, 1H, H^c), 8,79 (s, 2H, H^8), 8,54 (d, J = 7,8 Hz, 2H, H^3), 8,32 (dd, J = 8,3; 5,2 Hz, 1H, H^b), 8,23 (dd, J = 8,3; 0,8 Hz, 1H, H^h), 8,19 (d, J = 8,4 Hz, 2H, H^{12}), 8,07 (d, J =8,4 Hz, 2H, H^{11}), 7,97 (d, J = 8,4 Hz, 1H, H^l), 7,88 (m, 2H, H^4), 7,77 (d, J = 1,4 Hz, 1H, H^k), 7,71 (dd, J = 5,4; 1,1 Hz , 1H, H^j), 7,54 (d, J = 5,7 Hz, 2H, H^6) 7,29 (dd, J = 8,3; 5,1 Hz, 1H, H^i), 7,15 (dd, J = 7,2; 4,0 Hz, 2H, H^5). ^{13}C NMR (DMSO-d_6, 125,7 MHz, ppm): δ 164,7(C^9), 158,6(C^7), 158,2(C^2), 156,7(C^e), 152,3(C^a), 152,2(C^g), 151,8(C^i), 137,0(C^4), 136,3(C^c), 135,4(C^{11}), 128,6(C^{19}), 128,1(C^b), 127,8(C^{20}), 127,6(C^{12}), 127,6(C^{14}), 127,5(C^5), 126,9(C^{18}), 126,8(C^j), 126,5(C^{13}), 126,3(C^6), 126,3(C^{15}), 124,1(C^3), 123,8(C^d), 123,5(C^f), 110,5(C^8), 41,5(C^{10}). HRMS (ESI): m/z = 705,96 {[Ru(Brtrp)(phen)Cl]$^+$+H^+}.

9.3.2.3. Synthesis of [Ru(Brtrp)(dpa)Cl]Cl (5a"):

[Ru(Brtrp)Cl_3] **(4a)** (0.150 g, 0,252 mmol), 2,2'-dipyridylamine(0,043 g, 0,252mmol), LiCl (0,108 g, 2,52mmol), Et_3N (104 µL, 0,755 mmol), EtOH (22,5 mL), H_2O (7,5 mL).

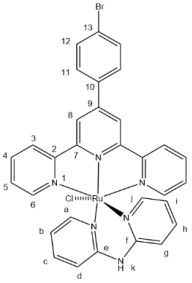

Dark red solid: Yield: 0,114 g (61,9 %). IR (KBr): 3470, 3394, 3158, 2954, 1628, 1467 cm^{-1}. ^1H NMR (DMSO-d_6, 500MHz, ppm): δ 10,61 (s, 1H, H^k), 9,43 (dd, J = 6,0; 1,9 Hz, 1H, H^a), 9,06 (s, 2H ,H^8), 8,89 (d, J = 7,8, 2H, H^3), 8,48 (dd, J = 5,6; 0,7 Hz, 2H, H^6), 8,42 (d, J = 6,8 Hz, 2H, H^{12}), 8,10 (m, 3H, H4 ; H^c), 7,88 (d, J = 6,8 Hz, 2H, H^{11}), 7,62 (dd, J = 7,2; 5,3 Hz, 2H, H^5), 7,50 (d, J = 8,1 Hz, 1H, H^d), 7,4 (dd, J = 8,8; 7,4 Hz, 2H, H^b), 7,35 (dd, J = 7,4; 6,0 Hz, 1H, H^h), 6,92 (d, J = 7,5 Hz, 1H, H^g), 6,59 (dd, J = 6,1; 1,7 Hz, 1H, H^i), 6,42 (dd, J = 6,8; 6,0 Hz, 1H, H^i). ^{13}C NMR (DMSO-d_6, 125,7 MHz, ppm): δ 159,5(C^e), 159,3(C^f), 155,0(C^7) 153,9(C^2), 153,4(C^a), 152,7(C^6), 149,0(C^j), 142,8(C^9), 138,6(C^c), 137,5(C^h), 137,0(C^4), 135,7(C^{10}), 132,33(C^{11}), 129,6(C^{12}) 127,4(C^5), 124,2(C^3), 123,5(C^{13}), 119,7(C^8), 118,9(C^i) 118,7(C^b), 114,0(C^d), 113,4(C^g). HRMS (ESI): m/z = 697,01 {[Ru(Brtrp)(dpa)Cl]$^+$+H^+}.

9.3.2.4. Synthesis of [Ru(Anitrp)(bipy)Cl]Cl (5b):

[Ru(Anitrp)Cl_3] **(4b)** (0.150 g, 0,282 mmol), 2,2'-bibyridine (0,044 g, 0,281 mmol), LiCl (0,120 g, 2,81 mmol), Et_3N (117 µL, 0,844 mmol), EtOH (22,5 mL), H_2O (7,5 mL).

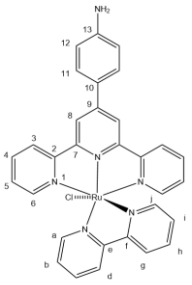

Dark red solid: Yield: 0,095 g (52,4%). IR (KBr): 3417, 1632, 1610, 1459, 1427, 1387 cm^{-1}. ^1H NMR (DMSO-d_6, 500MHz, ppm): δ 10,10 (dd, J = 5,4; 1,6 Hz, 1H, H^a), 9,06 (dd, J = 8,3; 1,0 Hz, 1H, H^d), 9,03 (s, 2H, H^8), 8,90 (dd, J = 8,2; 1,4 Hz, 2H, H^3), 8,69 (d, J = 5,5; 1,5 Hz, 2H, H^6), 8,21 (dd, J = 8,1; 1,0 Hz, 1H, H^g), 8,03 (dt, J = 7,6; 7,6; 1,8 Hz, 1H, H^c), 7,97 (td, J = 7,1; 5,8 Hz, 1H H^b), 7,96 (td, J = 7,7; 1,6 Hz, 2H, H^4), 7,67 (d, J = 8,6 Hz, 2H, H^{12}), 7,61 (t, J = 6,7; 5,4 Hz, 1H, H^i), 7,46 (m, 2H, H^5), 7,36 (t, 1H, H^h), 7,24 (t,1H, H^i), 6,90 (d, J = 8,6 Hz, 2H, H^{11}). HRMS (ESI): m/z = 288,27 {[Ru(Anitrp)(bipy)]$^{2+}$}.

9.3.2.5. Synthesis of [Ru(Anitrp)(phen)Cl]Cl (5b'):

[Ru(Anitrp)Cl_3] **(4b)** (0.150 g, 0,282 mmol), 1,10-phenantroline (0,052 g, 0,288 mmol), LiCl (0,120 g, 2,81 mmol), Et_3N (117 µL, 0,844 mmol), EtOH (22,5 mL), H_2O (7,5 mL).

Dark red solid: Yield: 0,095 g (52,4%). IR (KBr): 3417, 1632, 1610, 1459, 1427, 1387 cm^{-1}. ^1H NMR (DMSO-d_6, 500MHz, ppm): δ 10,30 (dd, J = 5,4; 1,6 Hz, 1H, H^a), 9,09 (dd, J = 8,3; 1,0 Hz, 1H, H^d), 9,06

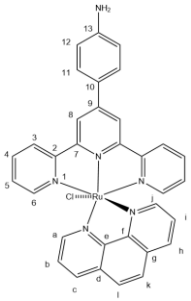

(s, 2H, H^8), 8,89 (d, J = 8,2; 1,4 Hz, 2H, H^3), HRMS (ESI): m/z = 288,27 {[Ru(Anitrp)(bipy)]$^{2+}$}.

9.3.2.6. Synthesis of [Ru(Ntrp)(bipy)Cl]Cl (5c):

[Ru(Ntrp)Cl_3] **(4c)** (0.150 g, 0,251 mmol), 2,2'-bibyridine (0,039 g, 0,252mmol), LiCl (0,108 g, 2,52mmol), Et_3N (104 µL, 0,755 mmol), EtOH (22,5 mL), H_2O (7,5 mL).

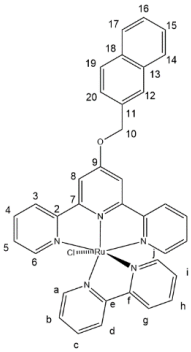

Dark red solid: Yield: 0,122 g (67,7%). IR (KBr): 3399, 3052, 1592, 1405, 1214, 760 cm^{-1}. ^{1}H NMR (DMSO-d_6, 500MHz, ppm): δ 10.07 (d, J = 5,4 Hz, 1H, H^a), 8,85 (d, J = 8,6 Hz, 1H, H^d), 8.72 (d, J = 8,2 Hz, 2H, H^3), 8.67 (s, 2H, H^8), 8,60 (d, J = 8,0 Hz, 1H, H^g), 8,30 (td, J = 7,3; 1,0 Hz, 1H, H^c), 8,20 (s, 1H, H^{12}), 8,07 (d, J = 8,5 Hz, 1H, H^{19}), 8,01 (m, 6H, H^4, H^{14}, H^{16}, H^{20}, H^b), 7,77 (d, J = 8,0 Hz, 2H, H^6), 7,61 (m, 3H, H^{15}, H^{17}, H^h), 7,44 (d, J = 5,5 Hz, 1H, H^i), 7,35 (dd, J = 7,7; 5,6 Hz, 2H, H^5), 7,09 (dd, J = 7,5; 6,0 Hz, 1H, H^i), 5,74 (s, 2H, H^{10}). HRMS (ESI): m/z = 682,17 {[Ru(Brtrp)(bipy)Cl]$^+$}.

9.3.3. General method for the synthesis of Ruthenium(II) complexes, [Ru(Brtrp)(*N,N*)(py)](PF$_6$)$_2$ (6) [29]:

In a light-protected flask at ambient temperature, the complexes [Ru(Brtrp)(*N,N*)Cl]Cl and the stoichiometric amount of $AgNO_3$ were dissolved in a MeOH/H_2O (4:1) mixture. The solution was stirred for 24 hours and afterwards the mixture was centrifuged to eliminate all the AgCl. Then, an excess of pyridine was added, and the reaction mixture was stirred again for 18 hours. The solution obtained was filtered and an excess of NH_4PF_6 and acetone were added. Slow evaporation of the solvent afforded a solid that was filtered.

9.3.3.1. Synthesis of [Ru(Brtrp)(bipy)(py)](PF$_6$)$_2$ (6a):

[Ru(Brtrp)(bipy)Cl]Cl **(5a)** (0,050 g, 0,070 mmol), $AgNO_3$ (0,024 g, 0,140 mmol), pyridine (70 µL), NH_4PF_6 (0,227 g, 1,39 mmol), acetone (1 mL).

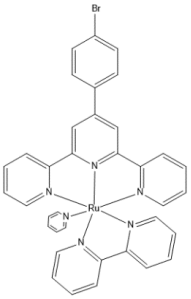

Dark red solid: Yield: 0,045 g (63,6%). IR (KBr): 2923, 2843, 1610, 1454, 1378, 840 cm^{-1}. HRMS (ESI): m/z = 323,49 {$[Ru(Brtrp)(bipy)]^{2+}$}.

9.3.3.2. Synthesis of $[Ru(Brtrp)(phen)(py)](PF_6)_2$ (6a'):

[Ru(Brtrp)(phen)Cl]Cl **(5a')** (0,050 g, 0,068 mmol), $AgNO_3$ (0,023 g, 0,135 mmol), pyridine (70 µL), NH_4PF_6 (0,220 g, 1,35 mmol), acetone (1 mL).

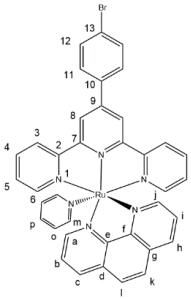

Dark red solid: Yield: 0,053 g (75,6%). IR (KBr): 3096, 2923, 1614, 1427, 836 cm^{-1}. ^1H NMR (CD_3OD, 500MHz, ppm): δ 9,20 (d, 1H, H^a), 9,08 (s, 2H, H^8), 8,98 (d, 2H, H^3), 8,81 (d, 2H, H^6), 8,79 (d, 1H ,H^k), 8,43 (d, 1H, H^h), 8,29 (dd, 1H, H^p), 8,24 (d, 1H, H^l), 8,11 (d, 2H, H^{11}), 8,08 8t, 2H, H^4), 7,92 – 7,85 (m, 5H, $H^{12,5,c}$), 7,74 (d, 1H, H^o), 7,65 (d, 1H, H^d), 7,53 (dd, 1H, H^b), 7,40 – 7,35 (m, 3H, $H^{m,j,g}$), 7,30 (t, 1H, H^i). HRMS (ESI): m/z = 334,47 {$[Ru(Brtrp)(phen)]^{2+}$}.

9.3.3.3. Synthesis of $[Ru(Brtrp)(dpa)(py)](PF_6)_2$ (6a''):

[Ru(Brtrp)(dpa)Cl]Cl **(5a'')** (0,050 g, 0,068 mmol), $AgNO_3$ (0,023 g, 0,137 mmol), pyridine (70 µL), NH_4PF_6 (0,223 g, 1,37 mmol), acetone (1 mL).

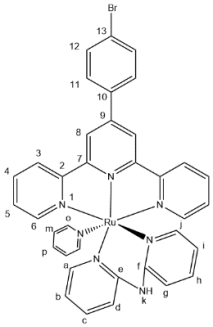

Dark red solid: Yield: 0,051 g (72,6%). IR (KBr): 3385, 3074, 2932, 2366, 1628, 1472, 840 cm^{-1}. ^1H NMR (DMSO-d_6, 500MHz, ppm): δ 10,73 (s, 1H, H^k), 9,19 (s, 2H, H^8), 9,01 (d, J = 8,0 Hz, 2H, H^3), 8,69 (d, J = 5,4 Hz, 2H, H^6), 8,26 (d, J = 8,6 Hz, 2H, H^{11}), 8,24 (td, J = 7,9; 1,9 Hz, 2H, H^4), 8,14 (t, J = 8,6 Hz, 1H, H^p), 7,91 (d, J = 8,6 Hz, 2H, H^{12}), 7,81 (d, J = 6,0 Hz, 1H, H^a), 7,75 (m, 2H, H^5), 7,73 (m, 1H, H^c), 7,67 (d, J = 5,2 Hz, 1H, H^o), 7,57 (d, J = 8,2 Hz, 1H, H^d), 7,53 (td, J = 7,2; 1,7 Hz, 1H, H^h), 7,26 (t, J = 7,2 Hz, 1H, H^b), 7,15 (t, J = 7,3 Hz, 1H, H^m), 7,01 (d, J = 7,3 Hz, 1H, H^g), 6,71 (d, J = 6,1 Hz, 1H, H^j), 6,57 (t, J = 6,6 Hz, 1H, H^i). ^{13}C NMR (DMSO-d_6, 125,7 MHz, ppm): δ 158,3($C^{e,f}$), 154,6(C^7), 154,3(C^2), 153,7(C^6), 152,2(C^a), 151,6(C^o), 149,6(C^g), 147,8(C^i), 144,8(C^{10}), 139,4(C^p), 138,8(C^h), 138,5(C^4), 137,9(C^c), 132,3(C^{12}), 129,6(C^{11}), 129,1(C^m),128,4(C^5), 125,3(C^3), 124,2(C^{13}), 121,1(C^8), 120,7(C^b), 119,3(C^i), 115,1(C^d), 114,0(C^g). HRMS (ESI): m/z = 329,98 {$[Ru(Brtrp)(dpa)]^{2+}$}.

9.3.4. Synthesis of $[Ru(Brtrp)_2](PF_6)_2$ (7a) [30]:

A little excess of Brtrp **(3a)** (0,167 g, 0,430 mmol) and a few drops (6 drops) of *N*-methylmorpholine were added to $RuCl_3 \cdot 3H_2O$ (0,050 g, 0,191 mmol) in 25 mL of MeOH. The mixture was refluxed for 8 hours under N2 atmosphere. The solution obtained was filtered and an excess of NH_4PF_6 (0,064 g, 0,392 mmol) was added to the filtrate and stirred for 10 minutes. Then the precipitate obtained was filtered and washed with MeOH.

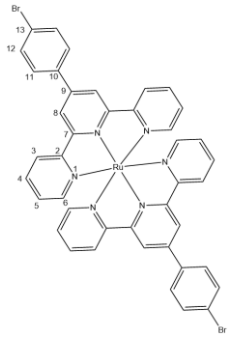

Dark red solid: Yield: 0,077 g (34,5%). IR (KBr): 3430, 1610, 1427, 1401, 1005 cm^{-1}. ^1H NMR (DMSO-d_6, 500 MHz, ppm): δ 9,47 (s, 2H, H^8), 9,04 (dd, J = 8,1; 0,8 Hz, 2H, H^3), 8,38 (d, J = 8,9 Hz, 2H, H^{12}), 8,04 (td, J = 8,4; 1,6 Hz, 2H, H^4), 7,97 (d, J = 8,9 Hz, 2H, H^{11}), 7,52 (dd, J = 5,3; 1,2 Hz, 2H, H^6), 7,25 (dd, J = 7,2; 5,1 Hz, 2H, H^5). ^{13}C NMR (DMSO-d_6, 125,7 MHz, ppm): δ 158,0(C^7), 155,2(C^2), 152,3(C^{12}), 145,6(C^{10}), 138,1(C^4), 135,3(C^9), 132,4(C^{11}), 129,7(C^6), 127,8(C^5), 124,9(C^3), 124,0(C^{13}), 121,0(C^8). HRMS (ESI): m/z = 438,83 $\{[Ru(Brtrp)_2]^{2+}\}$.

9.3.5. Synthesis of $[Ru(Brtrp)(Ntrp)](PF_6)_2$ (7b) [30]:

This complex was prepared by a procedure similar to the preparation of **7a** but using $[Ru(Brtrp)Cl_3]$ **(4a)** (0,102 g, 0,171 mmol) as starting material instead of $RuCl_3 \cdot H_2O$. A little excess of Ntrp **(3c)** (0,080 g, 0,200 mmol) and a few drops (6 drops) of *N*-methylmorpholine were added. The mixture was refluxed for 8 hours under N_2 atmosphere. The solution obtained was filtered and an excess of NH_4PF_6 (0,084 g, 0,513 mmol) was added to the filtrate and stirred for 10 min. Then the precipitate obtained was filtered and washed with MeOH.

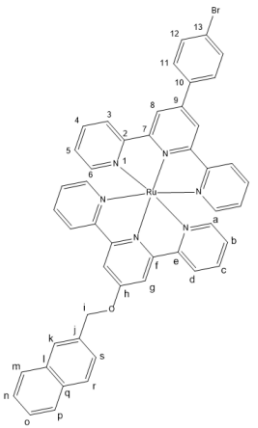

Red solid: Yield: 0,125 g (62,5%). IR (KBr): 3434, 1614, 1427, 1405, 1000 cm^{-1}. ^1H NMR (DMSO-d_6, 500 MHz, ppm): δ 9,47 (s, 2H, H^8), 9,05 (d, J = 8,3 Hz, 2H, H^d), 8,95 (s, 2H, H^g), 8,87 (d, J = 7,4 Hz, 2H, H^3), 8,38 (d, J = 8,7 Hz, 2H, H^6), 8,25 (s, 1H, H^k), 8,12 (d, J = 8,2 Hz, 1H, H^s), 8,06-7,99 (m, 6H, Hc, Ha, H^4), 7,97 (d, J = 5,5 Hz, 2H, H^{12}), 7,82 (dd, J = 8,8; 1,1 Hz, 1H, H^r), 7,62 (m, 1H, H^o), 7,55 (d, J = 5,5 Hz, 2H, H^{11}), 7,49 (d, J = 6,3 Hz, 1H, H^p), 7,31 (dd, J = 7,3; 5,2 Hz, 2H, H^b), 7,23 (dd, J = 7,1; 5,8 Hz, 2H, H^5), 5,8 (s, 2H, H^i). ^{13}C NMR (DMSO-d_6, 125,7 MHz, ppm): δ 165,7(C^h), 158,2(C^2), 157,9(C^7), 138,0(C^c), 132,5(C^4), 129,8(C^6), 128,7(C^s), 128,1(C^a), 127,9($C^{5,12}$), 127,6($C^{b,k}$), 126,8(C^o), 126,3(C^r), 124,9(C^3), 121,0(C^8), 111,6(C^g), 71,8(C^i). HRMS (ESI): m/z = 438,95 $\{[Ru(Brtrp)(Ntrp)]^{2+}\}$.

10. CONCLUSIONS

Four 4'-substituted-terpyridines ligands **(3a-d)** have been synthesized and characterized. These ligands have been reacted with $RuCl_3 \cdot 3H_2O$ to give four ruthenium (III) complexes [Ru(Rtrp)Cl_3] **(4a-d)**. The ruthenium complexes **4a-4c** have been reduced and reacted with a bidentate *N,N* ligand such as bipy, phen and dpa, to obtained the complexes [Ru(Brtrp)(*N,N*)Cl]Cl (*N,N* = bipy **(5a)**, phen **(5a')**, dpa **(5a")** and [Ru(Ntrp)(bipy)Cl]Cl (5c). The reaction of **5a**' or **5a"** with pyridine allows to obtain [Ru(Brtrp)(*N,N*)(py)]$(PF_6)_2$ (*N,N* = phen **(6a')**, dpa **(6a")**. Complexes with two terpyridines, one symmetric **(7a)** and one asymmetric **(7b)**, were also obtained. These complexes have been characterized by IR and NMR spectroscopy and mass spectrometry.

UV-Vis studies show that the maximum absorbance of the ruthenium (II) complexes is around 490-500 nm. These results have been used for posterior fluorescence studies where emission and excitation spectra have been recorded, confirming the fluorescent properties of the complexes.

The studies of the interaction of DNA with the complexes **5a** and **7a** by UV-Vis spectroscopy show a hypochromic and the bathochromic shifts of the absorbance maximum, that could indicate a covalent and intercalated interaction.

Moreover, electrophoresis shows the presence of these interactions in the non-irradiated samples and the excision of the DNA close to 100% in the samples irradiated with white light.

The conclusion of our work is that the complexes obtained have interesting photodynamic properties, which caused DNA fragmentation when activated by light. Biological studies with cells are necessary to estimate their capacity as an anticancer agent.

11. REFERENCES AND NOTES

1. H. Sung, J. Ferlay, R.L. Siegel, M. Laversanne, I. Soerjomataram, A. Jemal, F. Bray, CA A Cancer Journal for Clinicals**, 2021**, 71, 209-249.
2. M.J.Lind, Medicine, **2011**, 39, 711-716.
3. G. B. Kauffman, R. Pentimalli, S. Doldi, M. D. Hall, Platinum Metals Reviews, **2010**, 54, 250–256.
4. J. Reedijk, Proceedings of the National Academy of Sciences of the United States of America, **2003**, 100, 3611-3616.
5. R. Oun, Y. Moussa, N. Wheate**,** Dalton Transactions **2018**, 47, 6645-6653.
6. M. A. Skowron, M. Melnikova, J. G. H. van Roermund, A. Romano, P. Albers, J. Thomale, W. A. Schulz, G. Niegisch, M. J. Hoffmann, International Journal of Molecular Sciences, **2018**, 19, 1-17.
7. U. Ndagi, N. Mhlongo, M. E. Soliman, Drugs Design, Development and Therapy, **2017**, 11, 599-616.
8. M. J. Hannon, Pure and Applied Chemistry, **2007**, 79, 2243-2261.
9. E. J. Anthony, E. M. Bolitho, H. E. Bridgewater, O. W. L. Carter, J. M. Donnelly, C. Imberti, E. C. Lant, F. Lermyte, R. J. Needham, M. Palau, P. J. Sadler, H. Shi, F. X. Wang, W. Y. Zhang, Z. Zhang, Chemical Science, **2020**, 11, 12888-12917.
10. C. S. Allardyce, P. J. Dyson, Platinum Metals Reviews, **2001**, 45, 62-69.
11. L. Zeng, P. Gupta, Y. Chen, E. Wang, L. Ji, H. Chao, Z. S. Chen, Chemical Society Reviews, **2017**, 46, 5771−5804.
12. C. G. Hartinger, M. A. Jakupec, S. Zorbas-Seifrieda, M. Groessla, A. Eggera, W. Bergerd, H. Zorbas, P. J. Dyson, B. K. Keppler, Chemistry and Biodiversity, **2008**, 5, 2140-2155.
13. A. K. Bytzek, G. Koellensperger, B. K. Keppler, C. G. Hartinger, Journal of Inorganic Biochemistry, **2016**, 160, 250–255.
14. C. G. Hartinger, M. Groessl, S.I M. Meier, A. Casini, P. J. Dyson, Chemical Society Reviews, **2013**, 42, 6186—6199.
15. W. D. J. Tremlett, D. M. Goodman, T. R. Steel, S. Kumar, A. Wieczorek-Błauz, F. P. Walsh, M. P. Sullivan , M. Hanif, C. G. Hartinger, Coordination Chemistry Reviews, **2021**, 445, 213950.
16. S. Thota, D. A. Rodrigues, D. C. Crans, E. J. Barreiro Journal of Medicinal Chemistry, **2018,** 61, 5805−5821.

17. A. Bergamo, C. Gaiddon , J. H. M. Schellens, J.H. Beijnen , G. Sava, Journal of Inorganic Biochemistry, **2012**, 106, 90–99.
18. S. Monro, K. L. Colón, H. Yin, J. Roque, P. Konda, S. Gujar, R. P. Thummel, L. Lilge, C. G. Cameron, S. A. McFarland, Chemical Reviews, **2019**, 119, 797−828.
19. P. Kumar, S.Dasari, . K. Patra, European Journal of Medicinal Chemistry, **2017**, 136, 52-62.
20. Z. Huang, H. Xu, A. D. Meyers, A. I. Musani, L. Wang, R. Tagg, A. B. Barqawi, Y. K. Chen, Technology in Cancer Research and Treatment, **2008**, 7, 309-320.
21. C. Mari, V. Pierroz, S. Ferrariband, G. Gasser, Chemical Science**, 2015**, 6, 2660-86.
22. U.S.Schubert, C. Eschbaumer P. Andres, H. Hofmeier, C. H. Weidl, E. Herdtweck, E. Dulkeith, A. Morteani, N. E. Hecker , J. Feldmann, Synthetic Metals, **2001**, 121,1249-1252.
23. K. L. V. Joseph, A. Anthonysamy, R. Easwaramoorthi, D. V. Shinde, V. Ganapathy, S. Karthikeyan, J. Lee, T. Park, S. W. Rhee, K. S. Kim, J. K. Kim, Dyes Pigm. **2016**, 126, 270.
24. B. Liu, Y. Gao, M. A. Jabed, S. Kilina, G. Liu, W. Sun, ACS Applied Bio Materials, **2020**, 3, 9, 6025-6038.
25. M. M. Elnagar, S. Samir, Y. M. Shaker, A. A. Abdel-Shafi, W. Sharmoukh, M. S. Abdel-Aziz, K. S. Abou-El-Sherbini, Applied Organometallic Chemistry**, 2021**, 35, e6024.
26. J. Grau, R. F. Brissos, J. Salinas-Uber, A. B. Caballero, A. Caubet, O. Roubeau, L. Korrodi-Gregório, R. Pérez-Tomásc, P. Gamez, Dalton Transactions, **2015**, 44, 16061–16072.
27. M.M. Millutinovic, A. Rilak, I. Bratsos, O. Klisuric, M. Vranes, N. Gligorijevic, S. Radulovic, Z. D. Bugarcic, Journal of Inorganic Biochemistry, **2017**, 169, 1-12.
28. A. Habtemariam, M. Melchart, R. Fernández, S. Parsons, I. D. H. Oswald, A. Parkin, F. P. A. Fabbiani, J. E. Davidson, A. Dawson, R. E. Aird, D. I. Jodrell, P. J. Sadler, Journal of Medicinal Chemistry, **2006**, 49, 6858-6868.
29. G. Ragazzon, I. Bratsos, E. Alessio, L. Salassa, A. Habtemariam, R. J. McQuitty, G. J. Clarkson, P. J. Sadler, Inorganica Chimica Acta, **2012**, 393, 230-238.
30. T. Ezhilarasu, A. Sathiyaseelan, P. T. Kalaichelvan, S. Balasubramanian, Journal of Molecular Structure, **2017**, 1134, 265-277.
31. H. Zeng, C. Liu, M. Kira, Y. Segawa, Journal of Physics B: Atomic, Molecular and Optical Physics, **1999**, 32, L225-L230.
32. N. Shahabadi, S. Mohammadi, R. Alizadeh, Bioinorganic Chemistry and Applications, **2011**, 429241.

12. ACRONYMS

Cisplatin: *cis*- diamminedichloridoplatinum(II)

DNA: Deoxyribonucleic acid

ROS: Reactive oxygen species

PS: Photosensitizer

PDT: Photodynamic therapy

PACT: Photoactivated chemotherapy

MLCT: Metal-to-ligand charge transfer

trp: 2,2':6',2''-terpyridine

bipy: 2,2'-bipyridine

phen: 1,10-phenanthroline

dpa: Dipyridilamine

IR: Infrared

NMr: Nuclear Magnetic Resonance

UV-Vis: UltraViolet-Visible

APPENDICES

APPENDIX 1: IR

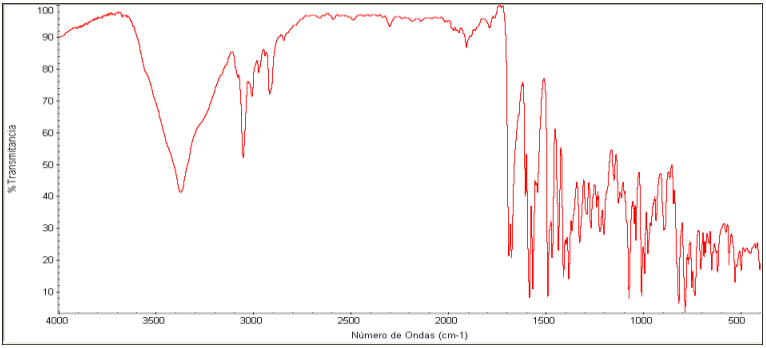

*Figure 22: IR (Brtrp) (**3a**).*

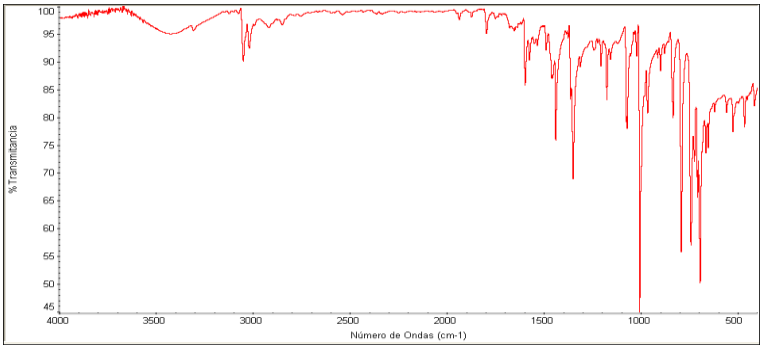

*Figure 23: IR [Ru(Brtrp)Cl_3] (**4a**).*

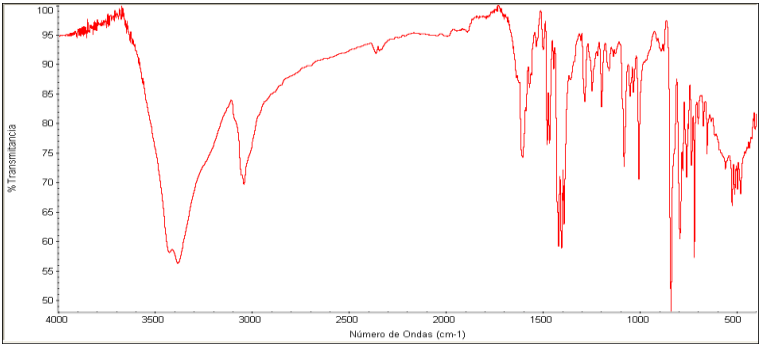

*Figure 24: IR [Ru(Brtrp)(phen)Cl]Cl (**5a'**).*

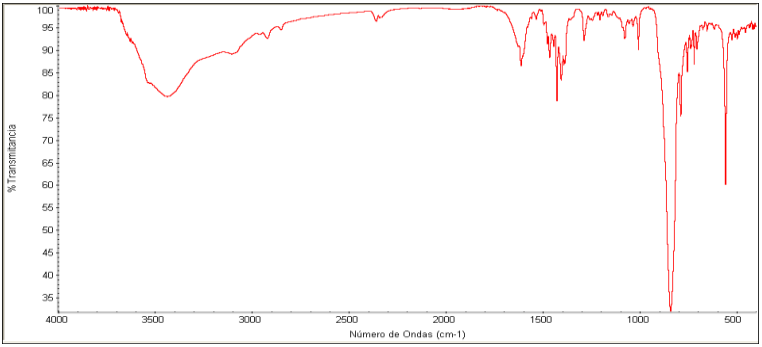

*Figure 25: IR [Ru(Brtrp)(phen)(py)]$(PF_6)_2$ (**6a'**).*

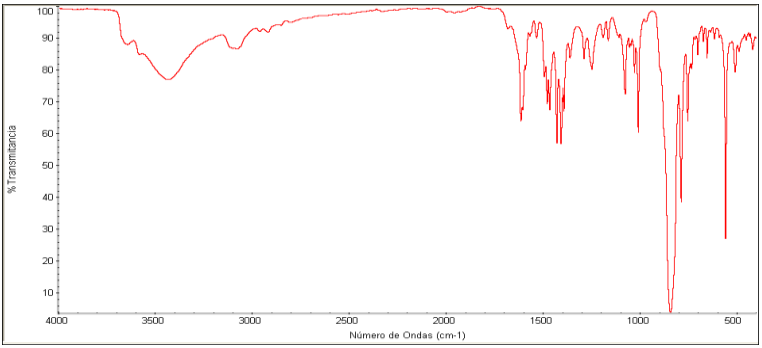

*Figure 26: IR [Ru(Brtrp)$_2$]$(PF_6)_2$ (**7a**).*

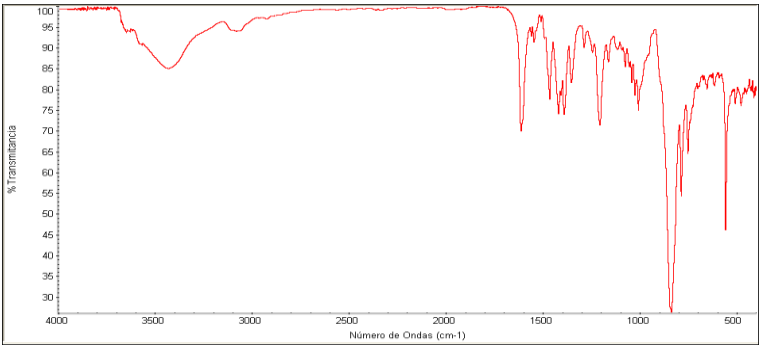

*Figure 27: IR [Ru(Brtrp)(Ntrp)][PF_6)$_2$ (**7b**).*

APPENDIX 2: MASS SPECTRA

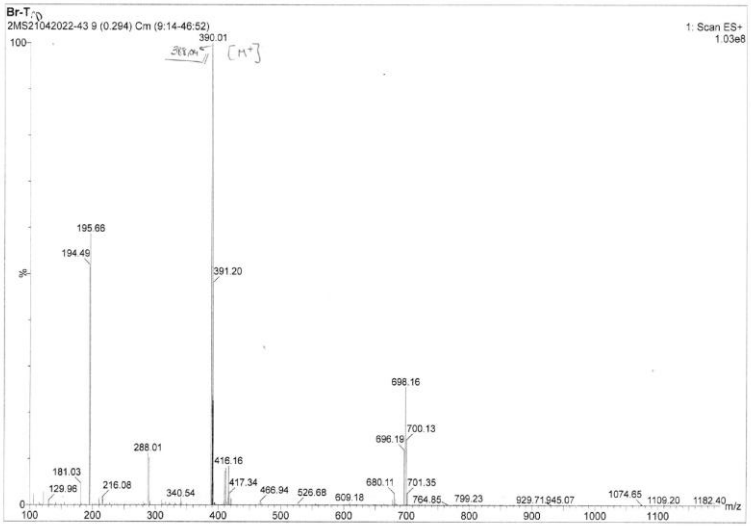

*Figure 28: MS (Brtrp) (**3a**).*

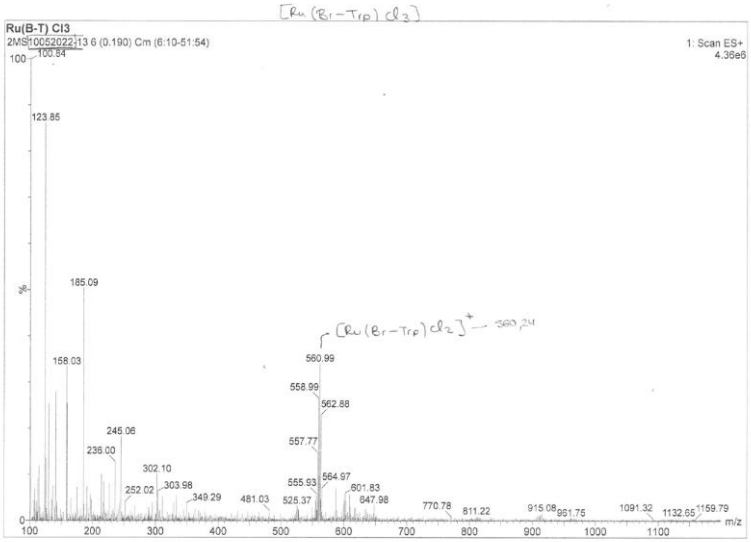

*Figure 29: MS [Ru(Brtrp)Cl₃] (**4a**).*

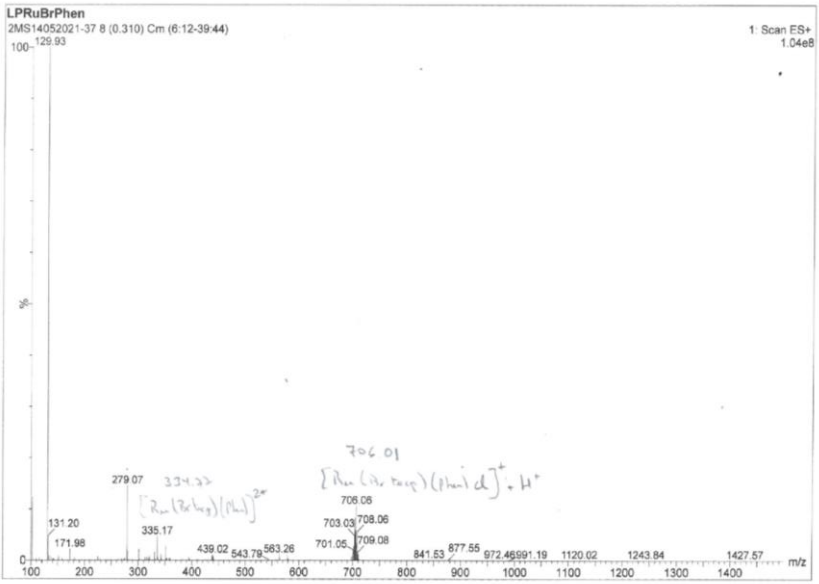

*Figure 30: MS [Ru(Brtrp)(phen)Cl]Cl (**5a'**).*

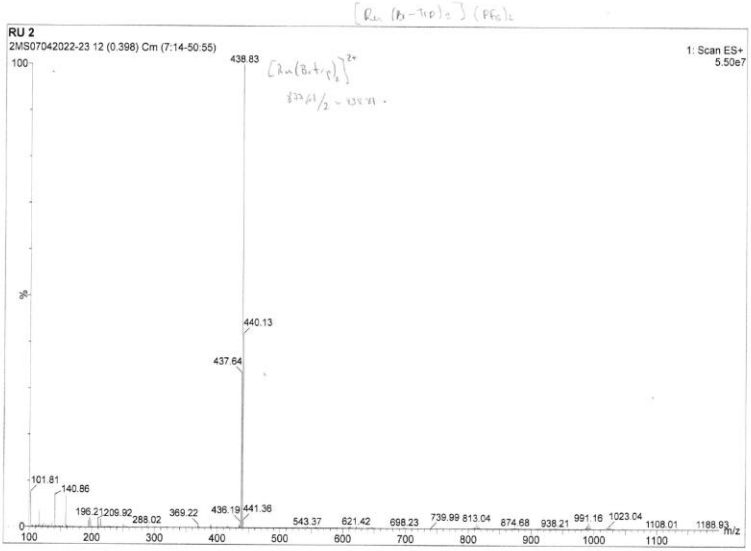

*Figure 31: MS [Ru(Brtrp)2](PF6)2 (**7a**).*

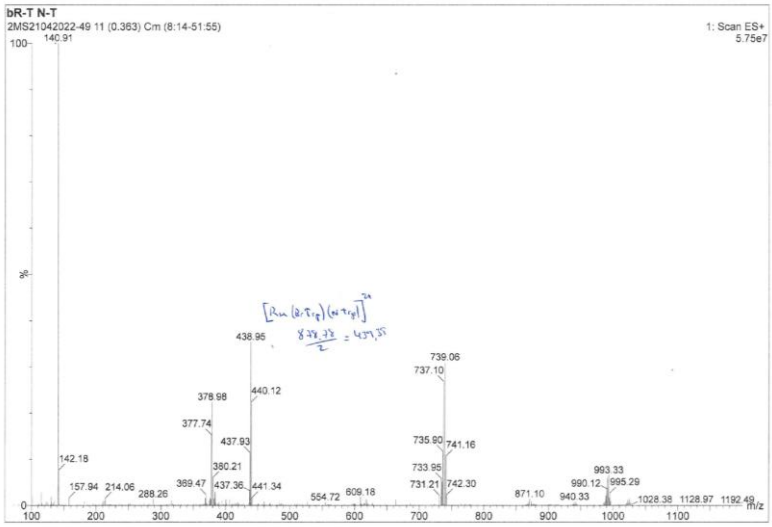

*Figure 32: MS [Ru(Brtrp)(Ntrp)](PF6)2 (**7b**).*

APPENDIX 3: RMN

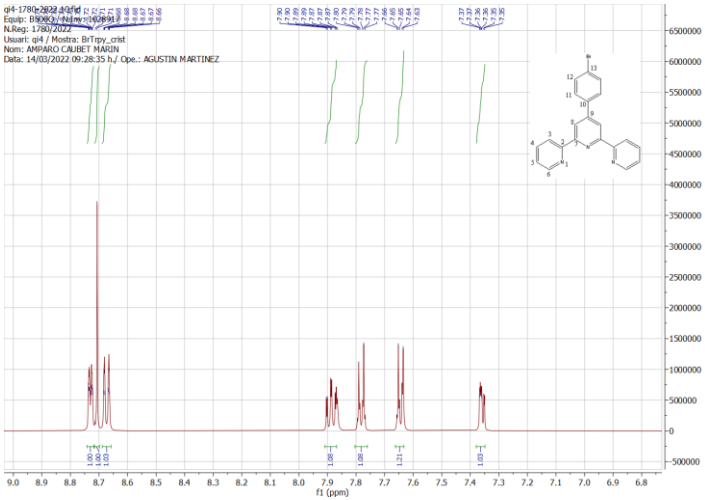

*Figure 33: RMN ^{1}H (Brtrp) (**3a**).*

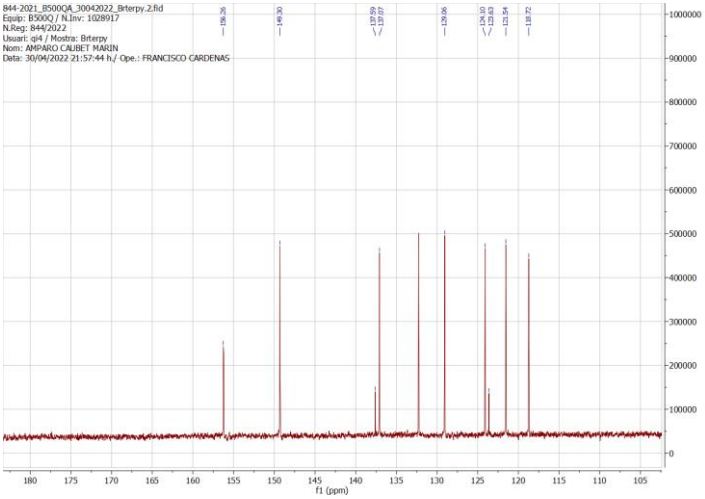

*Figure 34: RMN ^{13}C (Brtrp) (**3a**).*

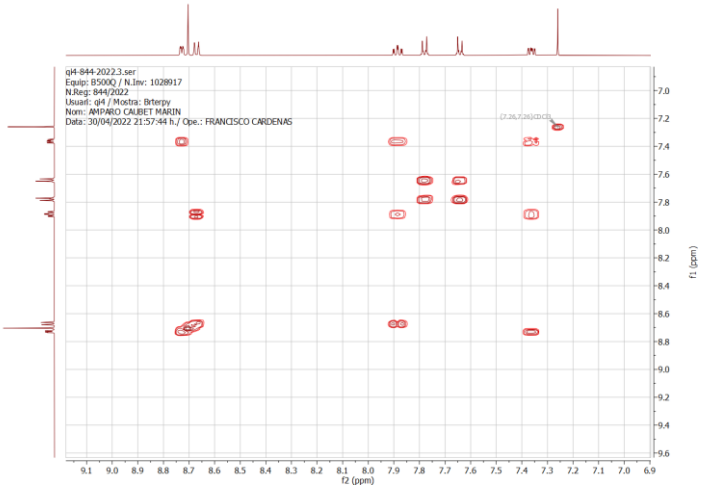

*Figure 35: Bidimensional NMR {^{1}H-^{1}H} COSY spectrum (Brtrp) (**3a**).*

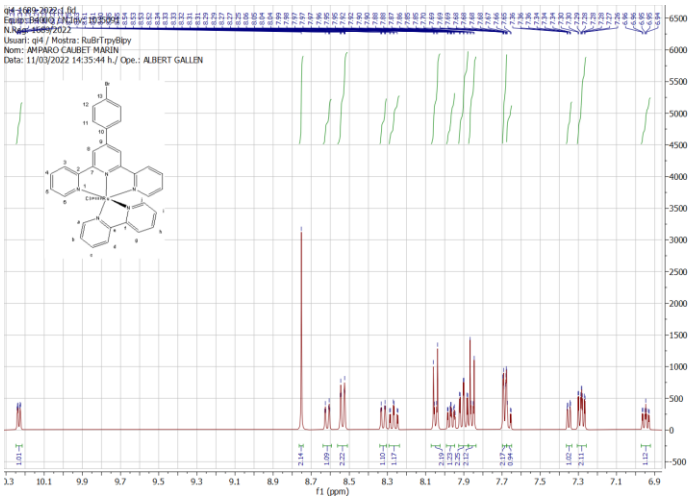

*Figure 36: RMN ^{1}H [Ru(Brtrp)(bipy)Cl]Cl (**5a**).*

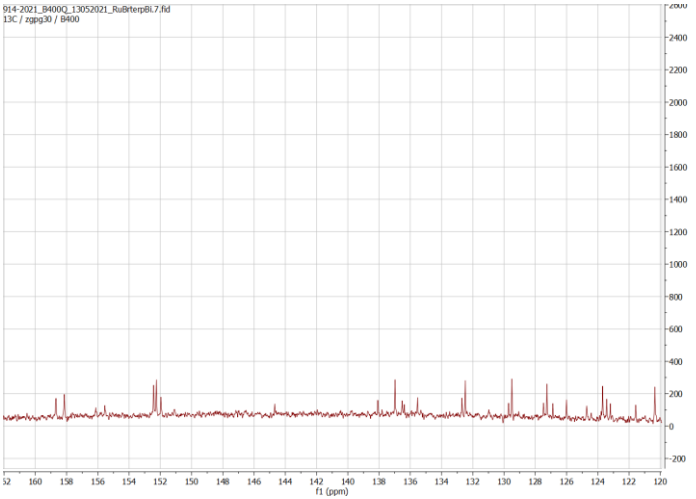

*Figure 37: ^{13}C [Ru(Brtrp)(bipy)Cl]Cl (**5a**).*

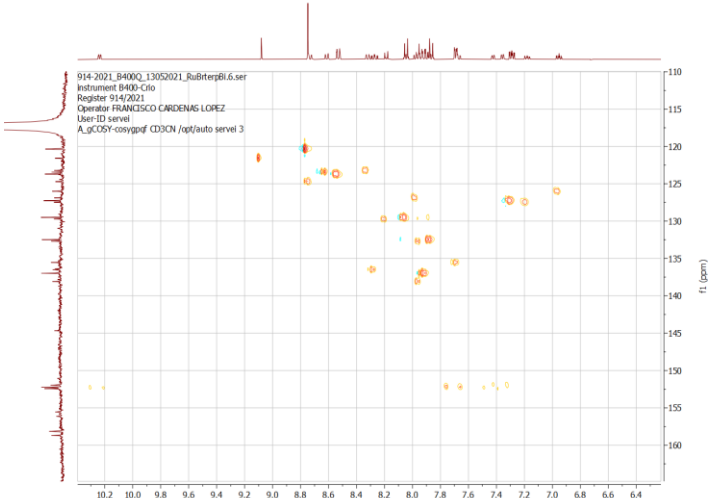

*Figure 38: Bidimensional NMR {^{1}H-^{13}C} HSQC spectrum [Ru(Brtrp)(bipy)Cl]Cl (**5a**).*

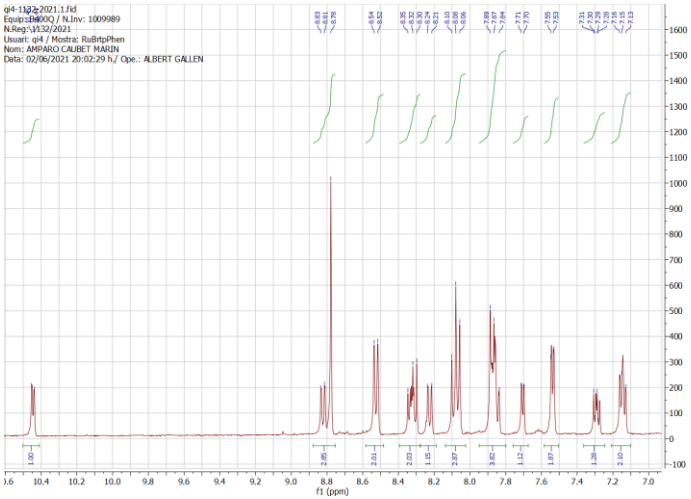

*Figure 39: [1]H [Ru(Brtrp)(phen)Cl]Cl (**5a'**).*

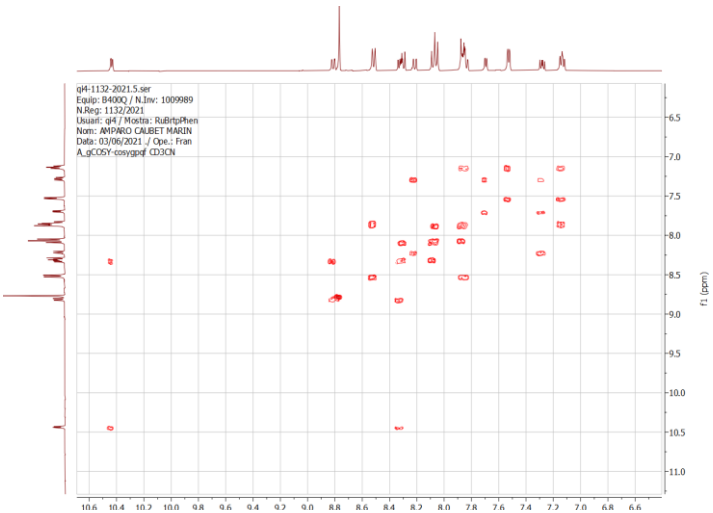

*Figure 40: Bidimensional NMR {[1]H-[1]H} COSY spectrum [Ru(Brtrp)(phen)Cl]Cl (**5a'**).*

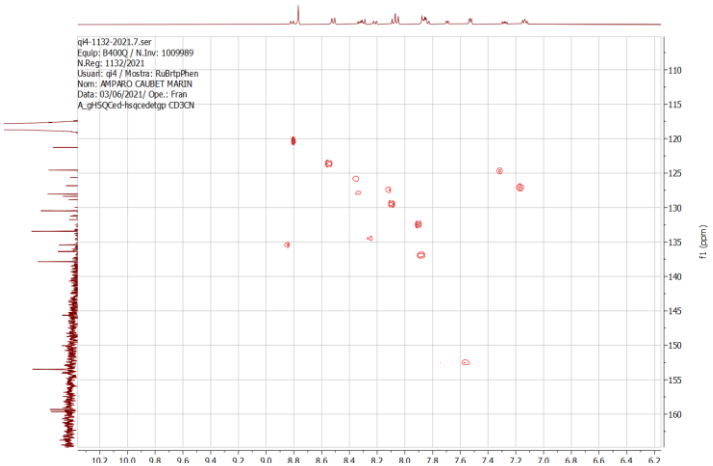

*Figure 41: Bidimensional NMR {^{1}H-^{13}C} HSQC spectrum [Ru(Brtrp)(phen)Cl]Cl (**5a'**).*

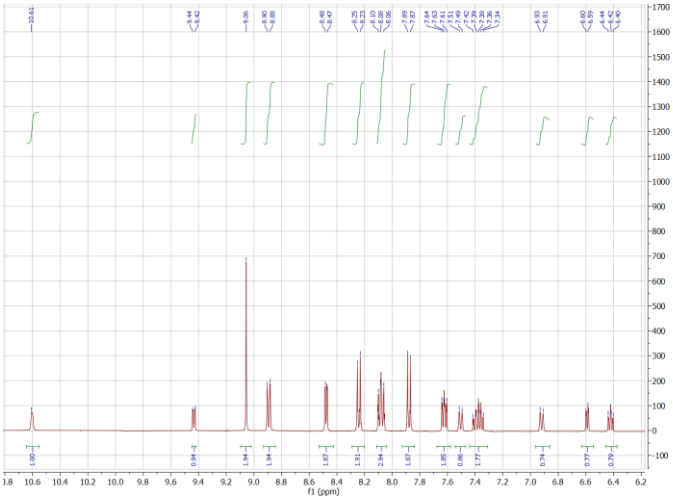

*Figure 42:^{1}H [Ru(Brtrp)(dpa)Cl]Cl (**5a"**).*

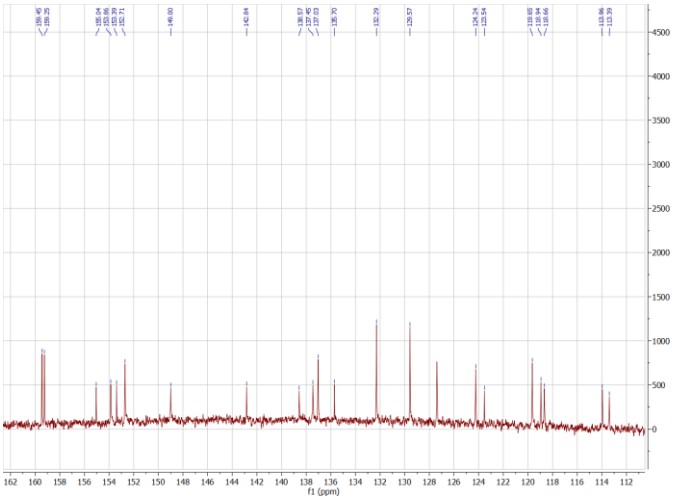

*Figure 43: ^{13}C [Ru(Brtrp)(dpa)Cl]Cl (**5a"**).*

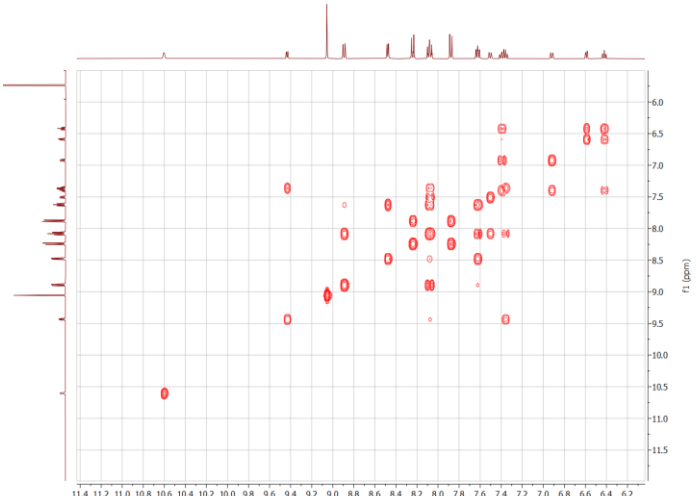

*Figure 44: Bidimensional NMR {^{1}H-^{1}H} COSY spectrum [Ru(Brtrp)(dpa)Cl]Cl (**5a"**).*

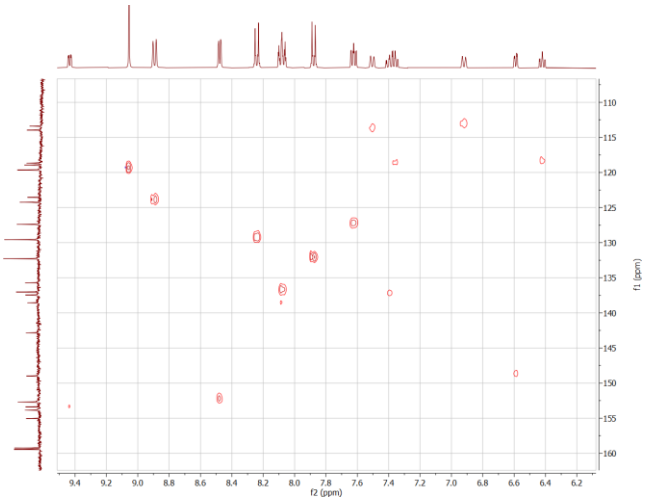

*Figure 45: Bidimensional NMR {^{1}H-^{13}C} HSQC spectrum [Ru(Brtrp)(dpa)Cl]Cl (**5a”**).*

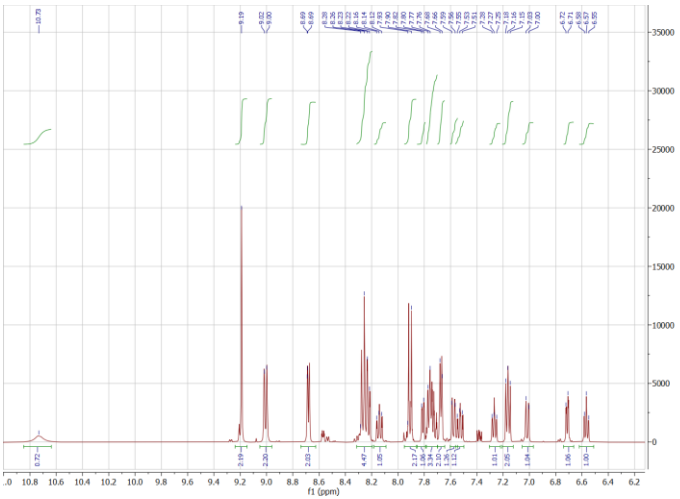

*Figure 46: ^{1}H [Ru(Brtrp)(dpa)(py)]$(PF_6)_2$ (**6a”**).*

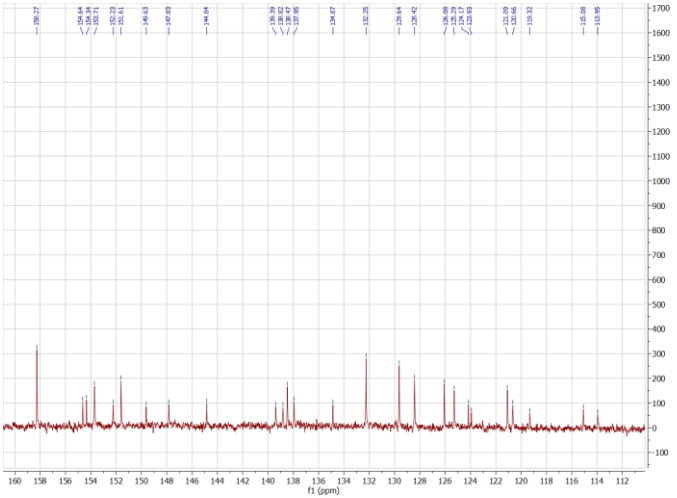

*Figure 47: ^{13}C [Ru(Brtrp)(dpa)(py)]$(PF_6)_2$ (**6a"**).*

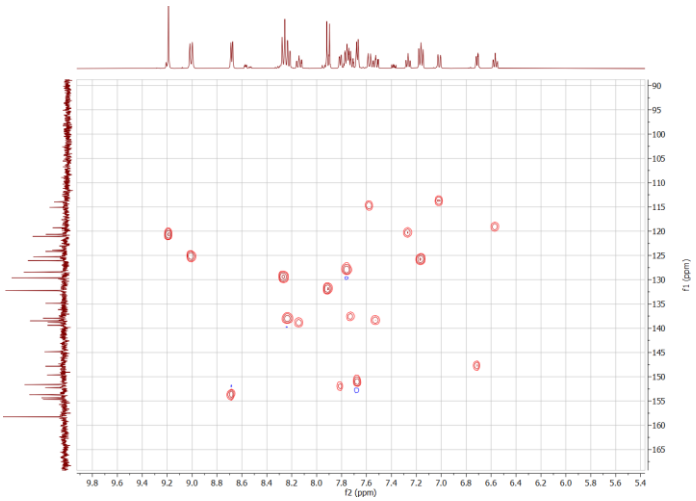

*Figure 48: Bidimensional NMR {^1H-^{13}C} HSQC spectrum [Ru(Brtrp)(dpa)(py)]$(PF_6)_2$ (**6a"**).*

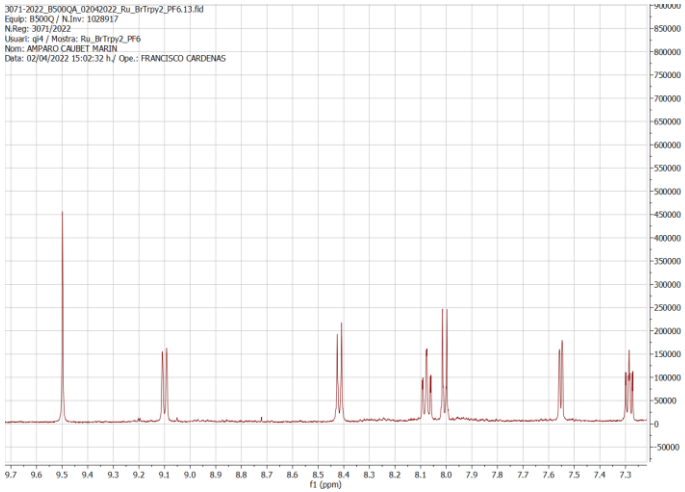

*Figure 49: ^{1}H $[Ru(Brtrp)_2](PF_6)_2$ (**7a**).*

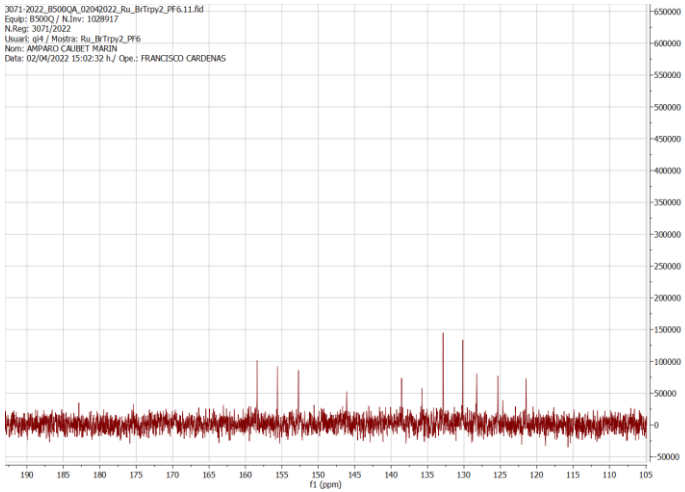

*Figure 50: ^{13}C $[Ru(Brtrp)_2](PF_6)_2$ (**7a**).*

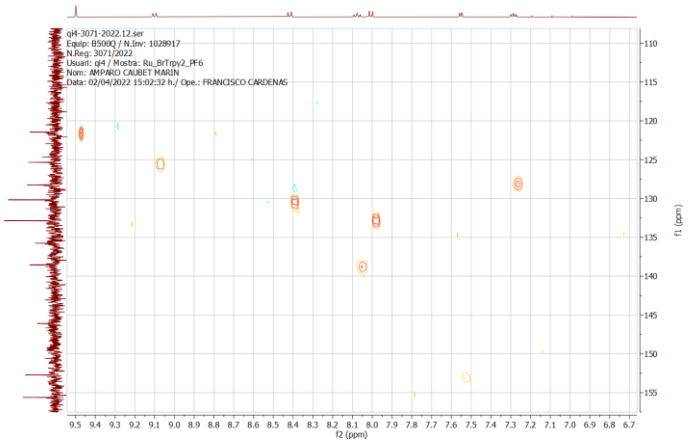

*Figure 51: Bidimensional NMR {^{1}H-^{13}C} HSQC spectrum $[Ru(Brtrp)_2](PF_6)_2$ (**7a**).*

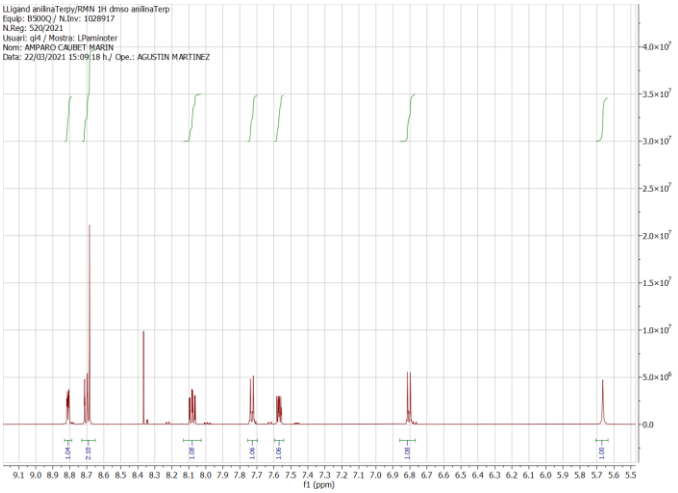

*Figure 52: ^{1}H (Anitrp) (**3b**).*

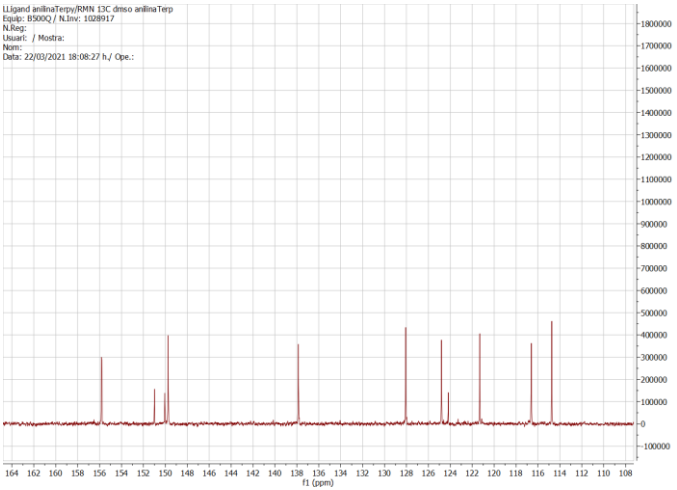

*Figure 53: ^{13}C (Anitrp) (**3b**).*

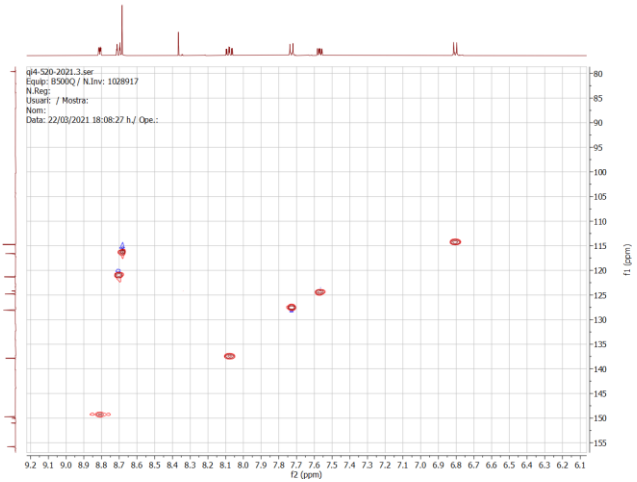

*Figure 54: Bidimensional NMR {^{1}H-^{13}C} HSQC spectrum (Anitrp) (**3b**).*

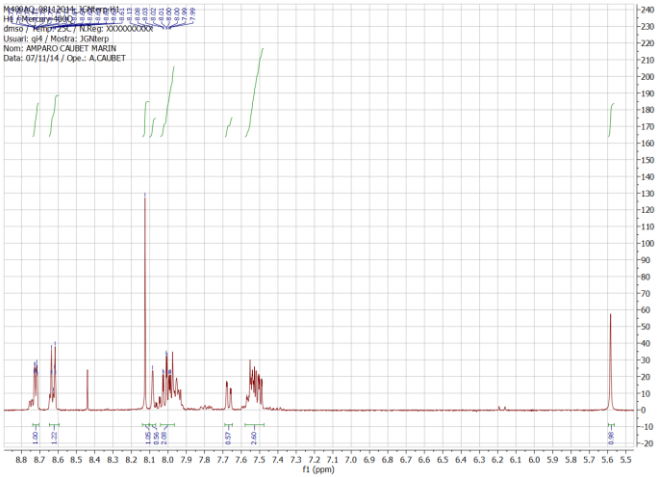

*Figure 55: [1]H (Ntrp) (**3c**).*

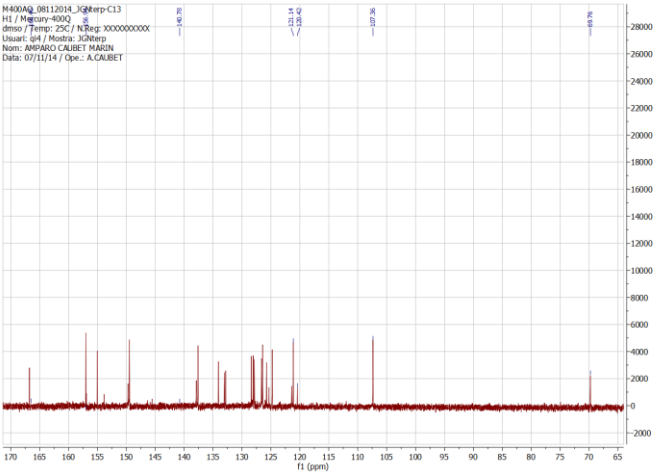

*Figure 56: [13]C (Ntrp) (**3c**).*

APPENDIX 4: UV-VIS AND FLUORESCENCE SPECTRA AND EXTINCTION COEFFICIENTS

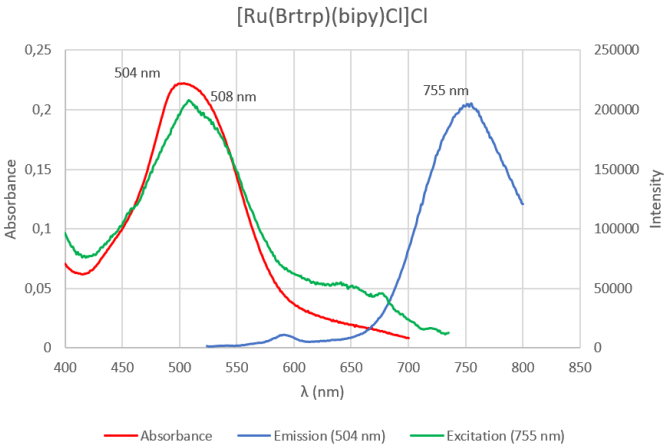

*Figure 57: Absorbance, Emission and Excitation (**5a**) 25µM in acetonitrile.*

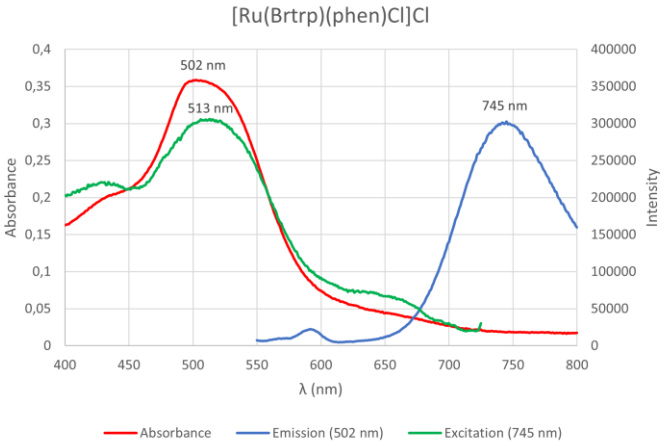

*Figure 58: Absorbance, Emission and Excitation (**5a'**) 25µM in acetonitrile.*

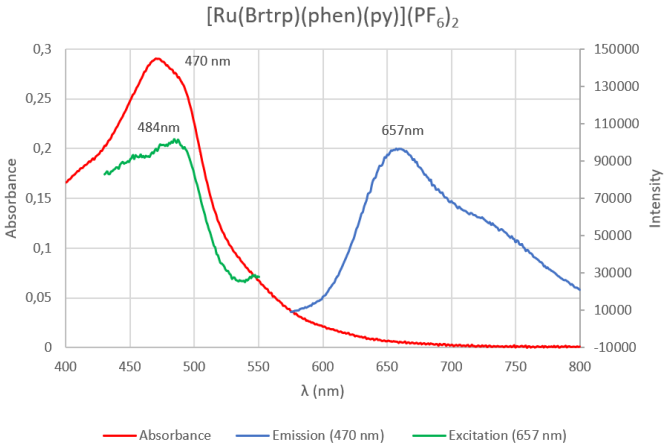

*Figure 59: Absorbance, Emission and Excitation (**6a'**) 25µM in acetonitrile.*

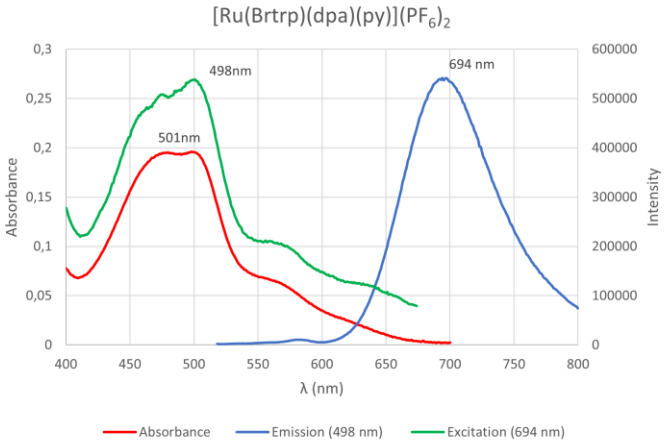

*Figure 60: Absorbance, Emission and Excitation (**6a''**) 25µM in acetonitrile.*

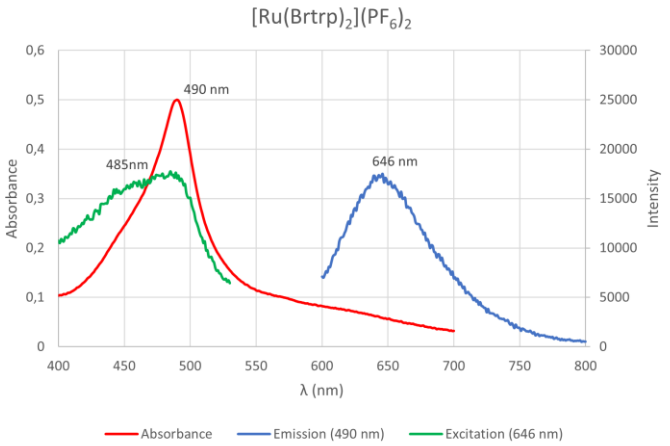

*Figure 61: Absorbance, Emission and Excitation (**7a**) 25μM in acetonitrile.*

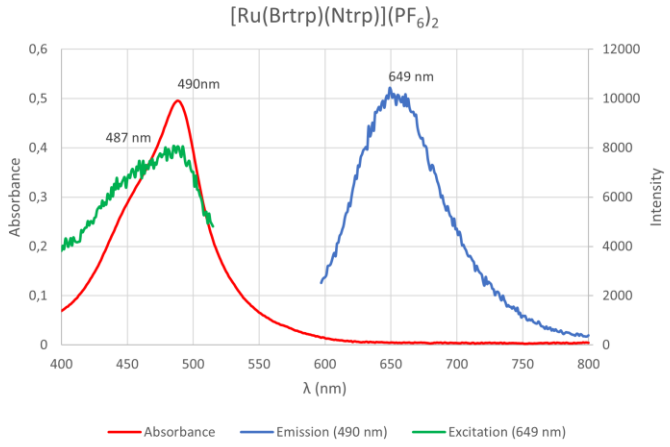

*Figure 62: Absorbance, Emission and Excitation (**7b**) 25μM in acetonitrile.*

Table 1: Wavelength and molar absorption constant.

Complex	λ (nm)	ε (M-1·cm-1)
5a	504	8,90E+03
5a'	472	1,23E+04
6a'	502	1,43E+04
5a''	514	8,79E+03
6a''	498	7,84E+03
5c	507	1,12E+04
7a	490	2,00E+04
7b	488	1,98E+04

APPENDIX 5: UV-VIS STUDIES

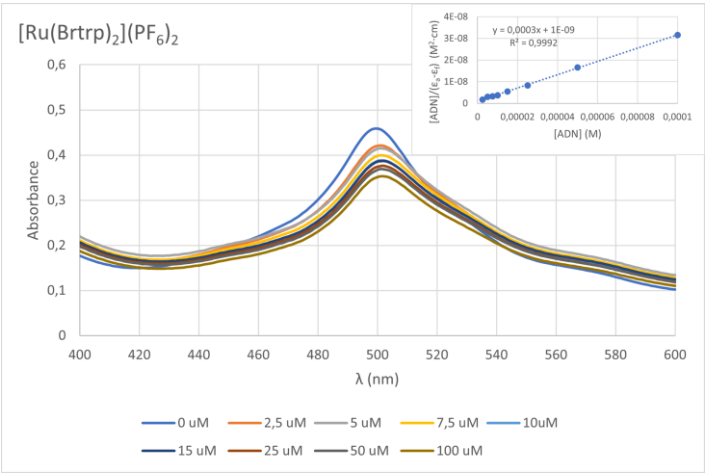

*Figure 63: UV-Vis spectra of (**7a**) and [DNA]]/(εa- εf) vs. [DNA].*